necrosis factor-α (TNF-α) and TNF-related apoptosis-inducing ligand differentially modulate proliferation and apoptotic pathways in human keratinocytes expressing the human papillomavirus-16 E7 oncoprotein. J Biol Chem 2001;276:22522–8.
7. Chen G, Goeddel Dv. TNF-R1 signaling: a beautiful pathway. Science 2002;296:1634–5.
8. Mundt AJ, Vijayakumar S, Nemunaitis J, et al. A Phase I trial of TNFerade biologic in patients with soft tissue sarcoma in the extremities. Clin Cancer Res 2004;10:5747–53.
9. Senzer N, Mani S, Rosemurgy A, et al. TNFerade biologic, an adenovector with a radiation-inducible promoter, carrying the human tumor necrosis factor α gene: a phase I study in patients with solid tumors. J Clin Oncol 2004;22:592–601.
10. Deveraux QL, Roy N, Stennicke HR, et al. IAPs block apoptotic events induced by caspase-8 and cytochrome *c* by direct inhibition of distinct caspases. EMBO J 1998;17:2215–23.
11. Roy N, Deveraux QL, Takahashi R, Salvesen GS, Reed JC. The c-IAP-1 and c-IAP-2 proteins are direct inhibitors of specific caspases. EMBO J 1997;16:6914–25.
12. Sidoti-De Fraisse C, Rincheval V, Risler Y, Mignotte B, Vayssiere JL. TNF-α activates at least two apoptotic signaling cascades. Oncogene 1998;17:1639–51.
13. Cappuzzo F, Magrini E, Ceresoli GL, et al. Akt phosphorylation and gefitinib efficacy in patients with advanced non-small-cell lung cancer. J Natl Cancer Inst 2004;96:1133–41.
14. Kulik G, Carson JP, Vomastek T, et al. Tumor necrosis factor α induces BID cleavage and bypasses antiapoptotic signals in prostate cancer LNCaP cells. Cancer Res 2001;61:2713–9.
15. Liu ZG, Hsu H, Goeddel DV, Karin M. Dissection of TNF receptor 1 effector functions: JNK activation is not linked to apoptosis while NF-κB activation prevents cell death. Cell 1996;87:565–76.
16. Argast GM, Campbell JS, Brooling JT, Fausto N. Epidermal growth factor receptor transactivation mediates tumor necrosis factor-induced hepatocyte replication. J Biol Chem 2004;279:34530–6.
17. Chen WN, Woodbury RL, Kathmann LE, et al. Induced autocrine signaling through the epidermal growth factor receptor contributes to the response of mammary epithelial cells to tumor necrosis factor α. J Biol Chem 2004;279:18488–96.
18. Hirota K, Murata M, Itoh T, Yodoi J, Fukuda K. Redox-sensitive transactivation of epidermal growth factor receptor by tumor necrosis factor confers the NF-κ B activation. J Biol Chem 2001;276:25953–8.
19. Izumi H, Ono M, Ushiro S, Kohno K, Kung HF, Kuwano M. Cross talk of tumor necrosis factor-α and epidermal growth factor in human microvascular endothelial cells. Exp Cell Res 1994;214:654–62.
20. Wang D, Yang EB, Cheng LY. Modulation of EGF receptor by tumor necrosis factor-α in human hepatocellular carcinoma HepG2 cells. Anticancer Res 1996;16:3001–6.
21. Woodworth CD, Mcmullin E, Iglesias M, Plowman GD. Interleukin 1 α and tumor necrosis factor α stimulate autocrine amphiregulin expression and proliferation of human papillomavirus-immortalized and carcinoma-derived cervical epithelial cells. Proc Natl Acad Sci U S A 1995;92:2840–4.
22. Beg AA, Baltimore D. An essential role for NF-κB in preventing TNF-α-induced cell death. Science 1996;274:782–4.
23. Wang CY, Mayo MW, Baldwin AS, Jr. TNF-and cancer therapy-induced apoptosis: potentiation by inhibition of NF-κB. Science 1996;274:784–7.
24. Wang CY, Guttridge DC, Mayo MW, Baldwin AS, Jr. NF-κB induces expression of the Bcl-2 homologue A1/Bfl-1 to preferentially suppress chemotherapy-induced apoptosis. Mol Cell Biol 1999;19:5923–9.
25. Mora AL, Corn RA, Stanic AK, et al. Antiapoptotic function of NF-κB in T lymphocytes is influenced by their differentiation status: roles of Fas, c-FLIP, and Bcl-xL. Cell Death Differ 2003;10:1032–44.
26. Kane LP, Shapiro VS, Stokoe D, Weiss A. Induction of NF-κB by the Akt/PKB kinase. Curr Biol 1999;9:601–4.
27. Rothe M, Pan MG, Henzel WJ, Ayres TM, Goeddel DV. The TNFR2-TRAF signaling complex contains two novel proteins related to baculoviral inhibitor of apoptosis proteins. Cell 1995;83:1243–52.
28. Wang CY, Mayo MW, Korneluk RG, Goeddel DV, Baldwin AS, Jr. NF-κB antiapoptosis: induction of TRAF1 and TRAF2 and c-IAP1 and c-IAP2 to suppress caspase-8 activation. Science 1998;281:1680–3.
29. Hoffmann M, Schmidt M, Wels W. Activation of EGF receptor family members suppresses the cytotoxic effects of tumor necrosis factor-α. Cancer Immunol Immunother 1998;47:167–75.
30. Lynch TJ, Bell DW, Sordella R, et al. Activating mutations in the epidermal growth factor receptor underlying responsiveness of non-small-cell lung cancer to gefitinib. N Engl J Med 2004;350:2129–39.
31. Paez JG, Janne PA, Lee JC, et al. EGFR mutations in lung cancer: correlation with clinical response to gefitinib therapy. Science 2004;304:1497–500.
32. Bianco R, Shin I, Ritter CA, et al. Loss of PTEN/MMAC1/TEP in EGF receptor-expressing tumor cells counteracts the antitumor action of EGFR tyrosine kinase inhibitors. Oncogene 2003;22:2812–22.
33. Ono M, Hirata A, Kometani T, et al. Sensitivity to gefitinib (Iressa, ZD1839) in non-small cell lung cancer cell lines correlates with dependence on the epidermal growth factor (EGF) receptor/extracellular signal-regulated kinase 1/2 and EGF receptor/Akt pathway for proliferation. Mol Cancer Ther 2004;3:465–72.
34. Sordella R, Bell DW, Haber DA, Settleman J. Gefitinib-sensitizing EGFR mutations in lung cancer activate anti-apoptotic pathways. Science 2004;305:1163–7.
35. Arao T, Fukumoto H, Takeda M, Tamura T, Saijo N, Nishio K. Small in-frame deletion in the epidermal growth factor receptor as a target for ZD6474. Cancer Res 2004;64:9101–4.
36. Prenzel N, Fischer OM, Streit S, Hart S, Ullrich A. The epidermal growth factor receptor family as a central element for cellular signal transduction and diversification. Endocr Relat Cancer 2001;8:11–31.
37. Rosenkranz S, Kazlauskas A. Evidence for distinct signaling properties and biological responses induced by the PDGF receptor α and β subtypes. Growth Factors 1999;16:201–16.
38. Uddin S, Fish EN, Sher DA, Gardziola C, White MF, Platanias LC. Activation of the phosphatidylinositol 3-kinase serine kinase by IFN-α. J Immunol 1997;158:2390–7.
39. Li L, Thomas RM, Suzuki H, De Brabander JK, Wang X, Harran PG. A small molecule Smac mimic potentiates TRAIL- and TNFα-mediated cell death. Science 2004;305:1471–4.
40. Ferreira CG, Van Der Valk P, Span SW, et al. Assessment of IAP (inhibitor of apoptosis) proteins as predictors of response to chemotherapy in advanced non-small-cell lung cancer patients. Ann Oncol 2001;12:799–805.
41. Vaziri SA, Grabowski DR, Tabata M, et al. c-IAP1 is overexpressed in HL-60 cells selected for doxorubicin resistance: effects on etoposide-induced apoptosis. Anticancer Res 2003;23:3657–61.
42. De Graaf AO, De Witte T, Jansen JH. Inhibitor of apoptosis proteins: new therapeutic targets in hematological cancer? Leukemia 2004;18:1751–9.
43. Nachmias B, Ashhab Y, Ben-Yehuda D. The inhibitor of apoptosis protein family (IAPs): an emerging therapeutic target in cancer. Semin Cancer Biol 2004;14:231–43.
44. Blick M, Sherwin SA, Rosenblum M, Gutterman J. Phase I study of recombinant tumor necrosis factor in cancer patients. Cancer Res 1987;47:2986–9.
45. Chapman PB, Lester TJ, Casper ES, et al. Clinical pharmacology of recombinant human tumor necrosis factor in patients with advanced cancer. J Clin Oncol 1987;5:1942–51.
46. Creaven PJ, Brenner DE, Cowens JW, et al. A phase I clinical trial of recombinant human tumor necrosis factor given daily for five days. Cancer Chemother Pharmacol 1989;23:186–91.
47. Feinberg B, Kurzrock R, Talpaz M, Blick M, Saks S, Gutterman JU. A phase I trial of intravenously-administered recombinant tumor necrosis factor-α in cancer patients. J Clin Oncol 1988;6:1328–34.
48. Gamm H, Lindemann A, Mertelsmann R, Herrmann F. Phase I trial of recombinant human tumour necrosis factor α in patients with advanced malignancy. Eur J Cancer 1991;27:856–63.
49. Spriggs DR, Sherman ML, Michie H, et al. Recombinant human tumor necrosis factor administered as a 24-hour intravenous infusion. A phase I and pharmacologic study. J Natl Cancer Inst 1988;80:1039–44.
50. Kuroda K, Miyata K, Fujita F, et al. Human tumor necrosis factor-α mutant RGD-V29 (F4614) shows potent antitumor activity and reduced toxicity against human tumor xenografted nude mice. Cancer Lett 2000;159:33–41.
51. Kuroda K, Miyata K, Tsutsumi Y, et al. Preferential activity of wild-type and mutant tumor necrosis factor-α against tumor-derived endothelial-like cells. Jpn J Cancer Res 2000;91:59–67.

Element Array by Scanning X-ray Fluorescence Microscopy after *Cis*-Diamminedichloro-Platinum(II) Treatment

Mari Shimura,[1] Akira Saito,[4,8,9] Satoshi Matsuyama,[5] Takahiro Sakuma,[1] Yasuhito Terui,[3] Kazumasa Ueno,[5] Hirokatsu Yumoto,[5] Kazuto Yamauchi,[5] Kazuya Yamamura,[6] Hidekazu Mimura,[5] Yasuhisa Sano,[5] Makina Yabashi,[7] Kenji Tamasaku,[8] Kazuto Nishio,[2] Yoshinori Nishino,[8] Katsuyoshi Endo,[6] Kiyohiko Hatake,[3] Yuzo Mori,[6] Yukihito Ishizaka,[1] and Tetsuya Ishikawa[8]

[1]Department of Intractable Diseases, International Medical Center of Japan; [2]Pharmacology Division, National Cancer Center Research Institute; [3]Division of Clinical Chemotherapy, Cancer Chemotherapy Center, Japanese Foundation for Cancer Research, Tokyo, Japan; Departments of [4]Material and Life Science and [5]Precision Science and Technology, and [6]Research Center for Ultra-Precision Science and Technology, Graduate School of Engineering, Osaka University, Suita, Osaka, Japan; [7]SPring-8/Japan Synchrotron Radiation Research Institute and [8]SPring-8/Riken, Hyogo, Japan; and [9]Nanoscale Quantum Conductor Array Project, ICORP, Saitama, Japan

Abstract

Minerals are important for cellular functions, such as transcription and enzyme activity, and are also involved in the metabolism of anticancer chemotherapeutic compounds. Profiling of intracellular elements in individual cells could help in understanding the mechanism of drug resistance in tumors and possibly provide a new strategy of anticancer chemotherapy. Using a recently developed technique of scanning X-ray fluorescence microscopy (SXFM), we analyzed intracellular elements after treatment with *cis*-diamminedichloro-platinum(II) (CDDP), a platinum-based anticancer agent. The images obtained by SXFM (element array) revealed that the average Pt content of CDDP-resistant cells was 2.6 times less than that of sensitive cells, and the zinc content was inversely correlated with the intracellular Pt content. Data suggested that Zn-related detoxification is responsible for resistance to CDDP. Of Zn-related excretion factors, glutathione was highly correlated with the amount of Zn. The combined treatment of CDDP and a Zn(II) chelator resulted in the incorporation of thrice more Pt with the concomitant down-regulation of glutathione. We propose that the generation of an element array by SXFM opens up new avenues in cancer biology and treatment. (Cancer Res 2005; 65(12): 4998-5002)

Introduction

Cis-Diamminedichloro-platinum(II) (CDDP) is an effective anticancer agent, but tumor cells can become resistant after CDDP-based therapy (1). Detoxification of CDDP, an increase in DNA repair, and excretion of CDDP have been implicated as major factors contributing to CDDP resistance (1). Incorporated CDDP is excreted by several molecules, such as overexpressed P-glycoprotein (2), a zinc-related defense system that is regulated by increased intracellular glutathione (GSH; ref. 3), and the ATP-dependent glutathione S-conjugate export pump (GS-X pump), which plays a role in the vesicle-mediated excretion of GSH-CDDP conjugates from resistant cells (4). Recent reports suggest that minerals such as zinc (Zn) and copper (Cu), important for normal cellular functions (5), are involved in CDDP resistance (6, 7). The simultaneous monitoring of multiple numbers of cellular elements would be helpful in identifying the mechanism of drug resistance in a malignant cell. The recently developed technique of scanning X-ray fluorescence microscopy (SXFM; refs. 8, 9) has made it possible to detect elements of interest by a single measurement and give a profile of these elements at the single-cell level (termed an element array). To examine the efficacy of element array analysis, we analyzed elements before and after treatment with CDDP and compared the element profiles of CDDP-sensitive and CDDP-resistant cells. We showed that the Zn content has an inverse correlation with Pt incorporation owing to a positive linkage with glutathione (GSH), a Zn-dependent detoxification factor. The combined treatment with CDDP and *N,N,N,N*-tetrakis-(2-pyridylmethyl)-ethylenediamine (TPEN), a Zn (II)-chelator (10), increased Pt uptake with a concomitant reduction of intracellular GSH. We propose that the element array is a versatile method suitable for obtaining information about metals involved in drug metabolism and could contribute to a novel strategy for anticancer chemotherapy.

Materials and Methods

Element array analysis by scanning X-ray fluorescence microscopy. SXFM was set up at an undulator beamline, BL29XU, of the SPring-8 synchrotron radiation facility (11) by combining a Kirkpatrick-Baez–type X-ray focusing system (12, 13), an XY-scanning stage for sample mounting, and an energy-dispersive X-ray detector (SDD, Röntec, Co., Ltd.). Monochromatic X-rays at 15 keV for Pt *L*-line excitation were focused into a 1.5 μm (*H*) × 0.75 μm (*W*) spot with a measured flux of ~ 1×10^{11} photons/s. The focused X-rays simultaneously yielded the fluorescence of various chemical species in a small volume of sample cells, as shown in Fig. 1*A*. The fluorescence from each element was taken independently and did not overlap except for the Pt$L\alpha$ signal, which was contaminated by Zn$K\beta$ (Fig. 1*A*). This was corrected by subtraction, as described previously (8). In this study, we could also measure Pt$L\beta$ as a unique signal of Pt (Fig. 1*A*). After counts were collected for 4.0 to 8.5 seconds at each pixel of scanning, the detected counts were normalized by incident beam intensity. In addition to the mapping images, an elemental concentration per single cell was calculated from the integrated elemental intensity over the whole mapping image.[10]

Requests for reprints: Yukihito Ishizaka, Department of Intractable Diseases, International Medical Center of Japan, 1-21-1 Toyama, Shinjuku-ku, 162-8655 Tokyo, Japan. Phone/Fax: 81-3-5272-7527; E-mail: zakay@ri.imcj.go.jp.

[10] A. Saito et al., manuscript in preparation.

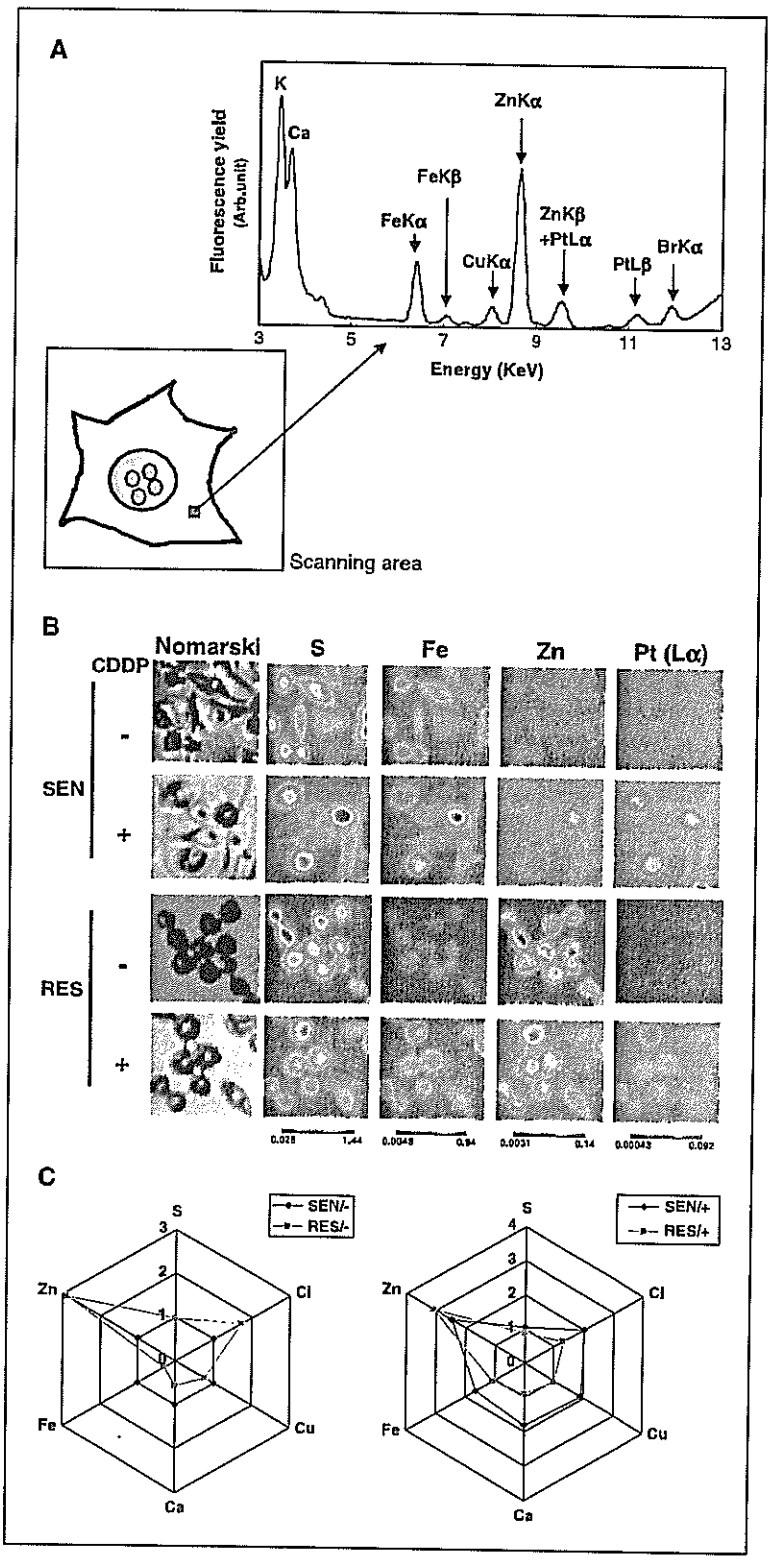

Figure 1. Element array by SXFM. *A*, scheme of imaging cellular elements by SXFM. Coherent X-rays are focused on each area (*pixel*), and the X-ray fluorescence from each element is detected. Each pixel gives an elemental spectrum, as shown in the right panel, and an integrated intensity of the individual element was mapped to the corresponding area of analyzed cells. *B*, SXFM analysis after CDDP treatment. Cell morphologies obtained by Nomarski are shown at ×100 magnification (*left*). Each field of view is equivalent to an area of 70 × 70 μm. Representative results are shown. Brighter colors indicate a higher signal intensity of each element. Results are shown for PC/SEN (*top*) and PC/RES cells (*bottom*). Note the high intensity of Pt*Lα* in PC/SEN cells after CDDP treatment (*second panel of the Pt column*) and the higher signal intensity of Zn in PC/RES cells compared with that of PC/SEN cells. *C*, element array based on SXFM analysis. The mean signal intensity of each element obtained by SXFM analysis was calculated, and the fold increase of elements in PC/RES cells (*red*) was depicted by using the intensity in PC/SEN cells (*blue*) as a standard (*left*). A part of analyzed elements is shown. The fold increase of elements in PC/SEN (*blue*) and PC/RES cells (*red*) after CDDP treatment was also shown by using the intensity in PC/SEN before CDDP treatment as a standard (*right*).

Chemicals and biochemical assays. TPEN (Sigma, St. Louis, MO; ref. 10), GSH (Calbiochem, La Jolla, CA), and CDDP (Daiichi Kagaku, Tokyo, Japan) were purchased. A GSH colorimetric assay kit (Calbiochem) and a BCA protein assay kit (Bio-Rad, Hercules, CA) were used for measuring intracellular GSH. About 3×10^5 to 4×10^5 cells were subjected to GSH measurement, and the data were normalized by cell number.

Cell lines. PC-9 cells (PC/SEN) and PC-9 cells resistant to CDDP (PC/RES), originally derived from a lung carcinoma cell line (14), were

maintained in DMEM (Nissui, Co., Tokyo, Japan) supplemented with 10% FCS (Sigma). The viability of PC/SEN cultured for 72 hours in the presence of 1 μmol/L CDDP was 40%, whereas that of PC/RES was ~90%. In this study, each cell line when treated with 1 μmol/L CDDP for 24 hours showed >85% viability.

Colony formation. After treatment, aliquots of PC/SEN and PC/RES were plated into culture dishes or soft agar, and the numbers of cell aggregates consisting of >50 cells were counted. Each number was normalized by plating efficiency, and the mean and SD of the number of formed colonies were calculated.

Sample preparation. Cells were plated on a silicon nitride base (NTT Advanced Technology, Tokyo, Japan) 1 day before the experiment. After incubation for 24 hours in the presence of 1 μmol/L CDDP, the cells were washed with PBS, fixed in 2% paraformaldehyde in PBS for 10 minutes at room temperature, and incubated in cold 70% ethanol for 30 minutes. The cells were then placed in a 1:3 solution of glacial acetic acid and methanol for 10 minutes, washed with 70% alcohol, and dried overnight at room temperature.

Measurement of cellular platinum and zinc. To measure Pt and Zn, ~5 × 10^6 cells were subjected to inductively coupled plasma mass spectroscopy (ICP-MS; Toray Research Center, Shiga, Japan; ref. 15).

Statistical analysis. The Pearson product-moment correlation coefficient and Student's *t* test were used to evaluate statistical significance (16).

Results and Discussion

Incorporation of platinum and element array after *cis*-diamminedichloro-platinum(II) treatment. We analyzed intracellular elements by SXFM after CDDP treatment (Fig. 1*A*). At 12 hours after treatment with 1 μmol/L CDDP, the level of Pt was increased in PC/SEN cells, whereas little increase in the Pt level was seen in PC/RES cells (Fig. 1*B*). The intensity of Pt in PC/RES cells was 2.6-fold less than that in PC/SEN cells, as confirmed by the results of ICP-MS, which indicated that the amount of Pt in PC/RES cells (5.5 fg/cell) was 3.6-fold less than that in PC/SEN cells (19.7 fg/cell). Therefore, the decreased accumulation of CDDP is likely to be responsible for resistance in PC/RES cells.

Based on the mean signal intensity obtained by SXFM, element array analysis was carried out (Fig. 1*C*). The element profile

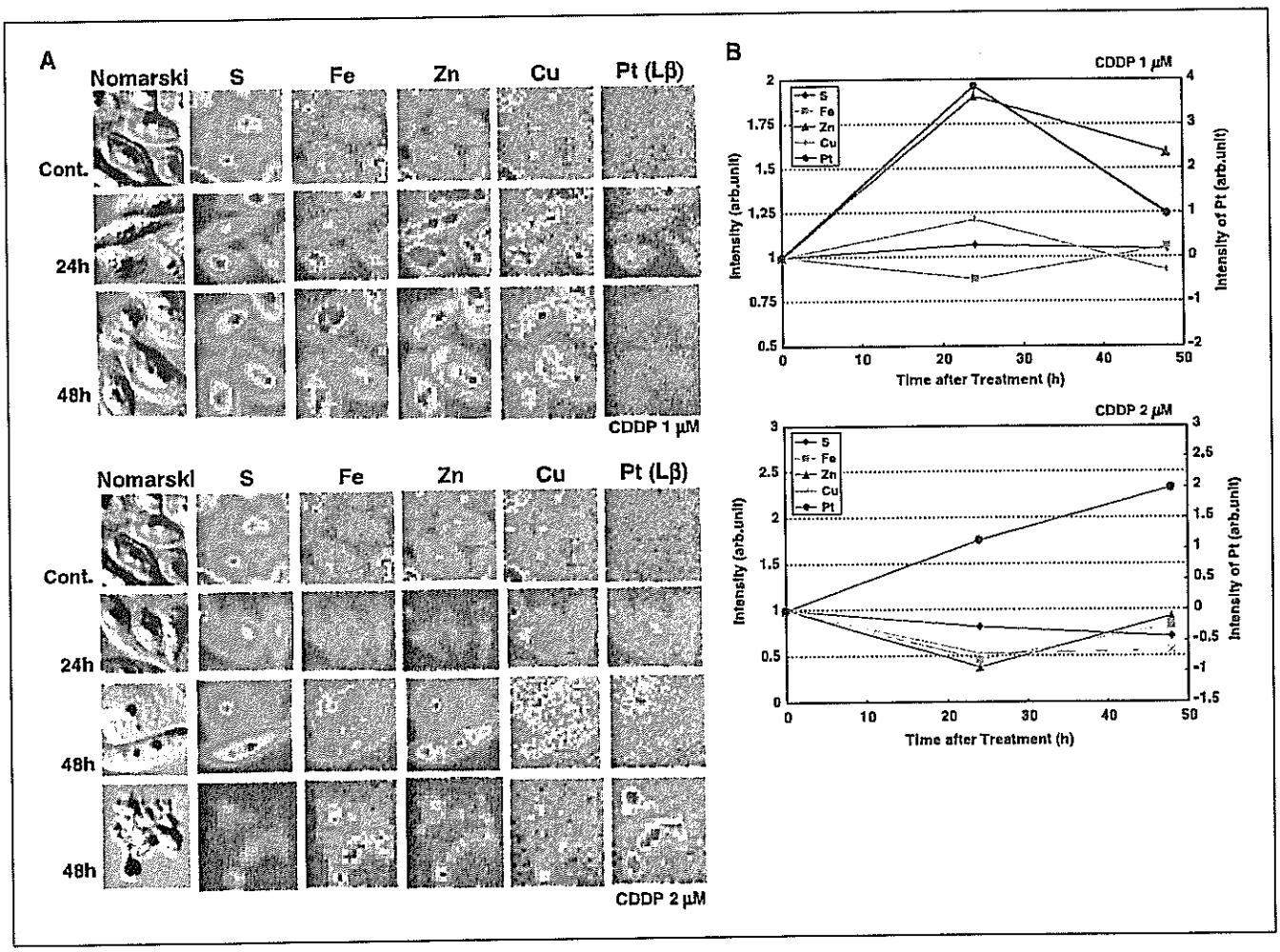

Figure 2. Chronological changes in elements after CDDP treatment. *A*, detection of elements in CDDP-treated PC/SEN cells. From the left, Nomarski images, signals of S, Fe, Zn, Cu, and Pt are shown. Top and bottom sets of panels show cells treated with 1 and 2 μmol/L CDDP, respectively. In each set of panels, control cells (*top*) and cells treated with CDDP for 24 hours (*middle*) and 48 hours (*bottom*) are shown. In this experiment, the signals of Pt*Lβ* were measured instead of Pt*Lα* (see Materials and Methods). The lowest panels show an apoptotic cell after 48 hours. *B*, summarized results of chronological changes of elements. The results after treatment with 1 μmol/L (*top*) and 2 μmol/L CDDP (*bottom*) are shown. The mean signal intensity was calculated from the results partly shown in (*A*). Among the cellular elements, Zn was most influenced by both 1 and 2 μmol/L CDDP treatment and had an inverse correlation with Pt content.

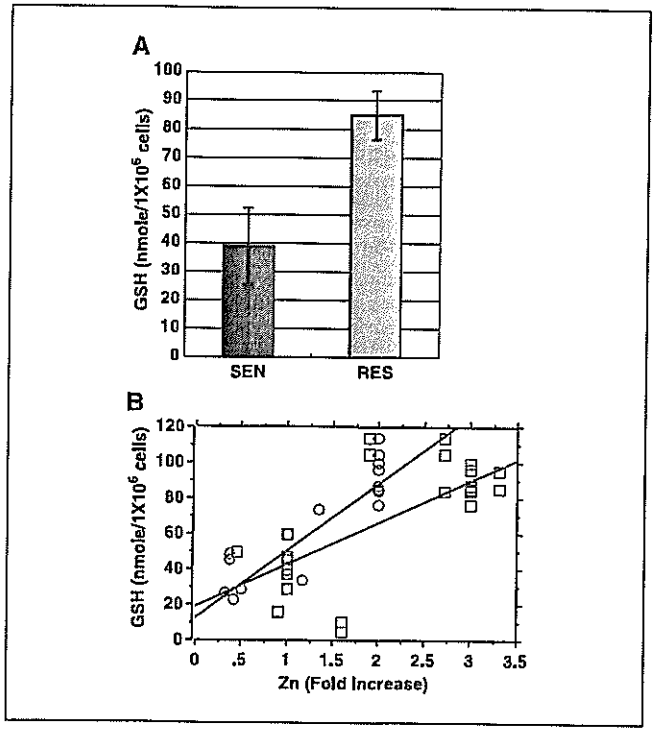

Figure 3. Cellular Zn content and GSH. *A*, basal level of intracellular GSH. The intracellular GSH levels in PC/SEN (*black*) and PC/RES cells (*gray*) were measured. GSH was significantly higher in PC/RES than in PC/SEN cells (*t* test, $P < 0.05$). *B*, correlation between Zn and intracellular GSH. A scatter diagram for Pearson product-moment correlation coefficient is depicted. Zn, measured by SXFM (*red squares*, $n = 27$) and by ICP-MS (*green circles*, $n = 29$), was plotted against intracellular GSH. Scattered values were based on data from both PC/SEN and PC/RES cells. The correlation coefficient *r* was calculated, and the statistical significance was determined ($P < 0.05$).

facilitates the identification of the elements related to the mechanism of drug resistance to CDDP. First, we noticed that the Zn content of untreated PC/RES cells was ~3-fold of that in PC/SEN cells (Fig. 1*C*, *left*). The difference in the Zn contents of these cells was confirmed by ICP-MS analysis (105 fg/cell for PC/SEN cells and 189 fg/cell for PC/RES cells, respectively). When 1 μmol/L CDDP was used for treatment, constitutive high Zn was observed in PC/RES (Fig. 1*C*, *right*). In PC/SEN cells, the amounts of all the elements were slightly increased, but the amount of Zn was increased most markedly.

We then analyzed the chronological changes in the levels of elements in PC/SEN cells following CDDP treatment. Representative results for S, Fe, Zn, Cu, and Pt are shown in Fig. 2*A*. Pt was clearly observed at 24 hours after treatment with 1 or 2 μmol/L CDDP (Fig. 2*A*). It was, however, barely detectable at 48 hours after the cells were treated with 1 μmol/L CDDP (Fig. 2*A*, *top*), suggesting that the cells excreted CDDP. In contrast, the cellular content of Pt gradually increased after treatment with 2 μmol/L CDDP (Fig. 2*A*, *bottom*), and apoptotic cells with high levels of incorporated CDDP were observed after 48 hours (Fig. 2*A*, *bottom*).

The element profile was plotted against the time after treatment with CDDP (Fig. 2*B*). When the cells were treated with 1 μmol/L CDDP, the Zn content increased remarkably and reached a peak at 24 hours (Fig. 2*B*, *top*, *red line*). In these cells, the Pt content was reduced after 48 hours. When the cells were treated with 2 μmol/L CDDP, the Zn content decreased within 24 hours (Fig. 2*B*, *bottom*), and the Pt content increased within 48 hours. In this analysis, Cu did not show significant changes. The results imply that the intracellular Zn content has an inverse correlation with the incorporated Pt content.

Cellular zinc and zinc-related detoxification. We studied Zn-related detoxification factors, such as metallothioneins (17), GSH (18), and the GSH-coupled excretory pump GS-X (4), and we observed that intracellular GSH was high in PC/RES cells (Fig. 3*A*). We then examined the possible correlation between the intracellular Zn content and GSH. As shown in Fig. 3*B*, the GSH levels showed a significant correlation with the levels of Zn detected by both ICP-MS and SXFM (Pearson product-moment correlation coefficient $r = 0.794$, $P < 0.05$ and $r = 0.533$, $P < 0.05$, respectively). The levels of Zn detected by SXFM may have less correlation with GSH than do the levels detected by ICP-MS because SXFM analyzed Zn in a small number of cells, whereas the analyses of GSH using ICP-MS were carried out on $>10^5$ cells.

Effects of zinc depletion and *cis*-diamminedichloroplatinum(II) uptake. To examine ways of increasing the sensitivity of PC/RES cells to CDDP, we used the Zn(II) chelator TPEN, as it was thought that CDDP uptake would increase when the GSH level was down-regulated by decreased Zn. Consistent with this hypothesis, treatment with 7.5 μmol/L of TPEN decreased cellular Zn to ~40 fg/cell at 30 hours after treatment in PC/SEN cells (Fig. 4*A*, *left*, *solid line*). The decrease seen in PC/RES cells owing to TPEN treatment was more rapid, with the Zn concentration being reduced to ~40 fg/cell within 7 hours (Fig. 4*A*, *left*, *dashed line*). The intracellular GSH also decreased with the reduction in intracellular Zn (Fig. 4*A*, *right*, *dashed line*).

To determine the effects of TPEN on the growth of PC/RES cells, the cells were pulse-treated for 2 hours with TPEN for 5 consecutive days and the growth was examined. Although treatment with 1 μmol/L CDDP did not induce apparent morphologic changes (Fig. 4*B*, *bottom*, *left*), the combined treatment with TPEN and CDDP caused prominent changes (Fig. 4*B*, *bottom*, *right*). A colony formation assay clearly showed that the combination of CDDP and TPEN, as well as single TPEN treatment, significantly impaired the growth of PC/RES cells (Fig. 4*C*). Consistent with these changes, ICP-MS indicated that the intracellular Pt content increased 3.5-fold after the combined treatment (from 0.38 to 1.35 fg/cell with TPEN treatment). It is important to note that the same dose of TPEN did not attenuate the growth of PC/SEN cells (Fig. 4*C*). These data indicate that the GSH level seems to be critical for resistance in PC/RES cells, consistent with previous reports that CDDP-resistant cells have high levels of GSH and that a decrease in GSH results in loss of resistance (3, 19). Our data also suggest that the high GSH content was maintained by the effects of Zn in PC/RES cells. Overall, our trial treatment with combined TPEN and CDDP suggests that this combination would be effective in eliminating tumors even if they include a CDDP-resistant population of cells with high Zn content.

We showed the use of element array analysis by SXFM to examine a mechanism of CDDP resistance. Based on element profiles, we successfully overcame CDDP resistance in PC/RES cells by using a Zn chelator that down-regulated the GSH level. Although it has been reported that Cu is a necessary factor for CDDP incorporation (7), the present work revealed that Cu was not involved in PC/RES cells. It is tempting to speculate that drug resistance is generated by various elements, and we propose that an element array can contribute to better understanding of cancer biology as well as other fields of medical science.

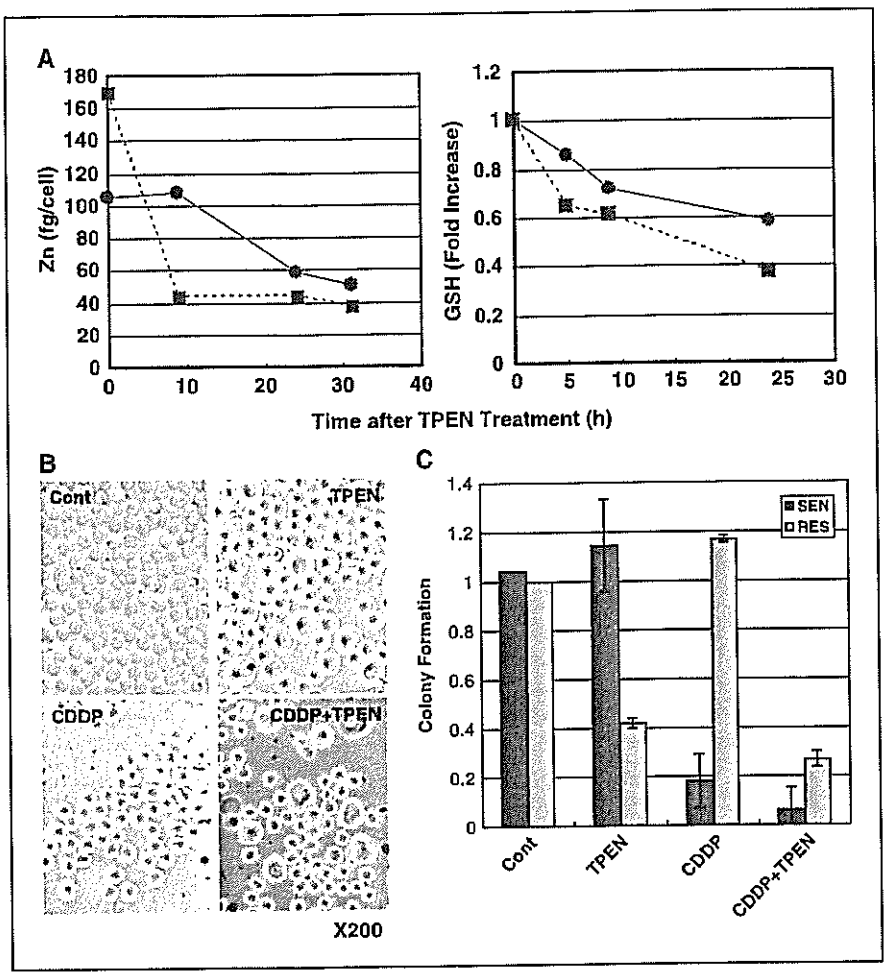

Figure 4. Cellular Zn content and Pt uptake with TPEN. *A*, TPEN-induced depletion of cellular Zn and down-regulation of GSH. TPEN (7.5 μmol/L) was added to the culture medium for the indicated time periods, and cellular Zn was measured by ICP-MS (*left*). Intracellular GSH content was also monitored (*right*). The Zn contents in PC/SEN (*solid lines*) and PC/RES cells (*dashed lines*) are shown. *B*, morphologic changes after pulse treatment with TPEN and CDDP. The morphologies of untreated PC/RES cells (*top*, *left*) and of cells treated with TPEN (*top*, *right*), CDDP (*bottom*, *left*), and CDDP plus TPEN (*bottom*, *right*) are shown. The cells were exposed to 1.0 μmol/L CDDP with or without 7.5 μmol/L TPEN for 2 hours, and then the medium was replaced with fresh medium. Pulse treatment was carried out for 5 consecutive days. Magnification, ×200. Note that large cells are observed after treatment with TPEN alone, and larger cells with irregular shape are observed following the combination treatment. The data showed that TPEN caused cellular accumulation at G_2-M phase with mitotic failure (data not shown). *C*, colony formation after pulse treatment with CDDP with or without TPEN. After pulse treatment for 5 consecutive days, as described in (*B*), the cells were plated in soft agar and the colony formation assay was done. The means and SDs of colony numbers of PC/SEN (*black columns*) and PC/RES cells (*gray columns*) are shown. The experiments were carried out in triplicate.

Acknowledgments

Received 2/3/2005; accepted 4/20/2005.

Grant support: Grant-in-aid for scientific research from the Ministry of Health, Labor, and Welfare of Japan and grant-in-aid for Center of Excellence Research (grant 08CE2004) from the Ministry of Education, Sports, Culture, Science, and Technology of Japan. The usage of BL29XU of the SPring-8 was supported by RIKEN.

The costs of publication of this article were defrayed in part by the payment of page charges. This article must therefore be hereby marked *advertisement* in accordance with 18 U.S.C. Section 1734 solely to indicate this fact.

We thank Harumi Shibata and Yasunori Suzuki for technical assistance.

References

1. Boulikas T, Vougiouka M. Cisplatin and platinum drugs at the molecular level. Oncol Rep 2003;10:1663–82.
2. Kuo TH, Liu FY, Chuang CY, Wu HS, Wang JJ, Kao A. To predict response chemotherapy using ^{99m}technetium tetrofosmin chest images in patients with untreated small cell lung cancer and compare with p-glycoprotein, multidrug resistance related protein-1, and lung resistance-related protein expression. Nucl Med Biol 2003;30:627–32.
3. Godwin AK, Meister A, O'Dwyer PJ, Huang CS, Hamilton TC, Anderson ME. High resistance to cisplatin in human ovarian cancer cell lines is associated with marked increase of glutathione synthesis. Proc Natl Acad Sci U S A 1992;89:3070–4.
4. Ishikawa T, Wright CD, Ishizuka H. GS-X pump is functionally overexpressed in *cis*-diamminedichloroplatinum (II)-resistant human leukemia HL-60 cells and down-regulated by cell differentiation. J Biol Chem 1994;269:29085–93.
5. Mayes PA, Nutrition. In: Murray RK, Granner DK, Mayers PA, Rodwell VW, editors. Harper's biochemistry. Chapter 54. 25th ed. New York: McGraw-Hill; 2000. p. 653–61.
6. Koropatnick J, Pearson J. Zinc treatment, metallothionein expression, and resistance to cisplatin in mouse melanoma cells. Somat Cell Mol Genet 1990;16:529–37.
7. Katano K, Kondo A, Safaei R, et al. Acquisition of resistance to cisplatin is accompanied by changes in the cellular pharmacology of copper. Cancer Res 2002;62:6559–65.
8. Ilinski P, Lai B, Cai Z, et al. The direct mapping of the uptake of platinum anticancer agents in individual human ovarian adenocarcinoma cells using a hard X-ray microprobe. Cancer Res 2003;63:1776–9.
9. Hall MD, Dillon CT, Zhang M, et al. The cellular distribution and oxidation state of platinum(II) and platinum(IV) antitumor complexes in cancer cells. J Biol Inorg Chem 2003;8:726–32.
10. Parat M-O, Richard M-J, Meplan C, Favir A, Béani J-C. Impairment of cultured cell proliferation and metallothionein expression by metal chelator *NNN' N'*-tetrakis-(2-pyridylmethyl)ethylene diamine. Biol Trace Elem Res 1999;70:51–68.
11. Miao J, Hodgson KO, Ishikawa T, Larabell CA, LeGros MA, Nishino Y. Imaging whole *Escherichia coli* bacteria by using single-particle X-ray diffraction. Proc Natl Acad Sci U S A 2003;100:110–2.
12. Kirkpatrick P, Baez AV. Formation of optical images by X-rays. J Opt Soc Am 1948;38:766–74.
13. Yamauchi K, Yamamura K, Mimura H, et al. Two-dimensional submicron focusing of hard X-rays by two elliptical mirrors fabricated by plasma chemical vaporization machining and elastic emission machining. Jpn J Appl Phys 2003;42:7129–34.
14. Kawamura-Akiyama Y, Kusaba H, Kanzawa F, Tamura T, Saijo N, Nishio K. Non-cross resistance of ZD0473 in acquired cisplatin-resistant lung cancer cell lines. Lung Cancer 2002;38:43–50.
15. Richarz AN, Wolf C, Bratter P. Determination of protein-bound trace elements in human cell cytosols of different organs and different pathological states. Analyst 2003;128:640–5.
16. Glantz SA. How to test for trends. In: Glantz SA, editor. Primer of biostatistics. Chapter 8. 2nd ed. New York: McGraw-Hill; 1987. p. 191–244.
17. Jourdan E, Jeanne RM, Régine S, Pascale G. Zinc-metallothinein genoprotective effect is independent of the glutathione depletion in HaCaT keratinocytes after solar light irradiation. J Cell Biochem 2004;92:631–40.
18. Parat M-O, Richard M-J, Béani J-C, Favier A. Involvement of zinc in intracellular oxidant/antioxidant balance. Biol Trace Elem Res 1997;60:187–204.
19. Hamaguchi K, Godwin AK, Yakushiji M, O'Dwyer PJ, Ozols RH, Hamilton TC. Cross-resistance to diverse drugs is associated with primary cisplatin resistance in ovarian cancer cell lines. Cancer Res 1993;53:5225–32.

Development and biological analysis of peritoneal metastasis mouse models for human scirrhous stomach cancer

Kazuyoshi Yanagihara,[1,6] Misato Takigahira,[1] Hiromi Tanaka,[1] Teruo Komatsu,[1] Hisao Fukumoto,[5] Fumiaki Koizumi,[5] Kazuto Nishio,[2] Takahiro Ochiya,[3] Yoshinori Ino[4] and Setsuo Hirohashi[4]

[1]Central Animal Laboratory; [2]Pharmacology Division; [3]Section for Studies on Metastasis; [4]Pathology Division, National Cancer Center Research Institute; and [5]Shien-Lab Medical Oncology Department, National Cancer Center Hospital, 5-1-1 Tsukiji, Chuo-ku, Tokyo 104-0045, Japan

(Received February 23, 2005/Accepted March 26, 2005/Online publication June 15, 2005)

The number of published studies on peritoneal dissemination of scirrhous gastric carcinoma is very small as a result of the unavailability of highly reproducible animal models. Orthotopic implantation of HSC-44PE and HSC-58 (scirrhous gastric carcinoma-derived cell lines) cells into nude mice led to dissemination of the tumor cells to the greater omentum, mesenterium, peritoneum and so on, and caused ascites in a small number of animals. Cycles of isolation of the ascitic tumor cells and orthotopic inoculation of these cells were repeated in turn to animals. This was to isolate highly metastatic cell lines with a strong capability of inducing the formation of ascites (44As3 from HSC-44PE; 58As1 and 58As9 from HSC-58). All three cell lines induced tumor formation at the site of orthotopic injection, and caused fatal cancerous peritonitis and bloody ascites in 90–100% of the animals approximately 3–5 weeks after the inoculation. When the parent cells were implanted, the animals became moribund in approximately 12–18 weeks, however, none of the animals developed ascites. Complementary DNA microarray and immunohistochemical analyses revealed differences in the expression levels of genes coding for the matrix proteinase, cell adhesion, motility, angiogenesis and proliferation between the highly metastatic- and parent-cell lines. The usefulness of this model for the evaluation of drugs was assessed by analyzing the stability of the metastatic potential of the cells and the reproducibility. Animals intravenously treated with CPT-11 and GEM showed suppressed tumor growth and significantly prolonged survival. The metastatic cell lines and the *in vivo* model established in the present study are expected to serve as a model of cancerous peritonitis developing from primary lesions, and as a useful means of clarifying the pathophysiology of peritoneal dissemination of scirrhous gastric carcinoma and the development of drugs for its treatment. (*Cancer Sci* 2005; 96: 323–332)

Although therapeutic results for gastric cancer have improved recently, the prognosis of patients with scirrhous gastric carcinoma still remains very poor. Scirrhous gastric carcinoma (diffusely infiltrative carcinoma or Borrmann's type-IV carcinoma, or the linitis plastica-type carcinoma) is characterized macroscopically by rigid thickening of the involved region of the gastric wall, causing it to assume a plate-like appearance, rather than by a well-defined mass.[1] Histopathologically, scirrhous cancer cells do not form glands, but cause diffuse infiltration of a broad region of the gastric wall, resulting in fibrous-like thickening of the gastric wall.[2,3] Because of such pathological features, early clinical diagnosis of scirrhous gastric carcinoma is difficult. By the time the diagnosis is made, peritoneal dissemination or distant metastasis to lymph nodes has already occurred in many cases. Peritoneal dissemination occurs frequently even after radical surgery, and is the cause of death in many patients.[4,5] Thus, peritoneal dissemination, a frequent form of recurrence and metastasis of scirrhous gastric carcinoma, serves as a major factor determining the prognosis of patients with scirrhous gastric carcinoma. To date, however, the mechanism of peritoneal dissemination in this type of cancer has not yet been fully elucidated.

Several theories have been proposed to explain the mechanism of peritoneal dissemination in human gastric cancer; it has been suggested that the cancer cells are detached from the primary lesions and freed into the peritoneal cavity, to colonize the peritoneum and induce cancerous peritonitis. However, most of the proposed theories remain speculations, and are seldom based on adequate evidence.[6–8] It cannot be overemphasized therefore that animal models of this condition are urgently needed to pursue studies on its pathophysiology. Some investigators have reported on a model of this condition established by direct inoculation of cultured gastric cancer cells into the peritoneal cavity.[9,10] It is difficult, however, to view this model as faithfully reflecting the characteristics of cancerous peritonitis observed in clinical cases. In the past, it was considered difficult to reliably establish a model of peritoneal dissemination developing from the primary lesions. Under these circumstances, we established seven cultured cell lines derived from human scirrhous gastric carcinoma and analyzed their characteristics.[11–14] Of these cell lines, the HSC-44PE and HSC-58 cells were found to show spontaneous metastasis to lymph nodes and lungs following s.c. implantation in nude mice.[14] Then, to isolate cell lines with a high metastatic potential, we performed repetitive s.c. inoculation of these cell lines and isolated sublines that tended to metastasize to lymph nodes. When these sublines were implanted orthotopically, a small number of animals showed massive bloody ascites. This phenomenon resembled the cancerous peritonitis seen in clinical cases and suggested a high possibility of establishing a reproducible mouse model of peritoneal dissemination.

In the present paper, we shall report on an analysis of the characteristics of tumor cell lines that often cause ascites (cell lines with a high potential for peritoneal dissemination) isolated by repeated orthotopic implantation of HSC-44PE and HSC-58 cells. The paper will also describe the results of cDNA microarray and immunohistochemical analyses of these cell lines as the first step towards clarifying the molecular mechanism of development of peritoneal metastasis in gastric cancer. In addition, the usefulness of these cell lines as a model for drug evaluation will also be discussed.

[6]To whom correspondence should be addressed. E-mail: kyanagih@gan2.res.ncc.go.jp
Abbreviations: cDNA, complementary DNA; CPT-11, camptothecin; GEM, gemcitabine; s.c., subcutaneously; i.p., intraperitoneally; i.v., intravenously.

 doi: 10.1111/j.1349-7006.2005.00054.x

Materials and Methods

Cell lines and culture. HSC-39, HSC-44PE and HSC-58 and cell lines established from human scirrhous gastric carcinomas have been reported previously.[11,14] The cell lines were maintained in RPMI1640 medium (Immuno-Biological Laboratories (IBL), Takasaki, Japan) supplemented with 10% FCS (Sigma Chemical, St. Louis, MO, USA), 100 IU/mL penicillin G sodium and 100 μg/mL streptomycin sulfate (IBL) in a 5% CO_2 and 95% air atmosphere at 37°C. The cells were passaged and expanded by trypsinization (0.05% trypsin and 0.02% EDTA; IBL), followed by replating every 5–7 days. All the cell lines were routinely tested for Mycoplasma by the Central Institute for Experimental Animals (Kawasaki, Japan), and no contamination was detected. For injection into mice, cells in log-phase growth were harvested by trypsinization and washed with serum-free RPMI1640 medium.

Animal experimentation. The animal experimental protocols were approved by the Committee for Ethics of Animal Experimentation, and the experiments were conducted in accordance with the Guidelines for Animal Experiments in the National Cancer Center. The mice were purchased from CLEA Japan (Tokyo, Japan) and maintained under specific pathogen-free conditions. They were provided with sterile food and water and housed in cages. The ambient light was controlled to provide regular 12-h light and 12-h darkness cycles.

Establishment of cell lines with a strong potential for inducing the formation of peritoneal metastasis. HSC-44PE and HSC-58 cell lines were inoculated by the orthotopic implantation technique into BALB/c nude mice. At appropriate intervals, or when moribund, the mice were sacrificed and the ascitic tumor cells were harvested aseptically. The cell suspensions were then cultured *in vitro*. The same procedure was repeated using both cell lines, and cell lines with a high potential for inducing the formation of peritoneal metastasis were established after 12 cycles of stepwise selection. Each resultant cell line after *in vitro* passages 5–10 was used for experiments.

Orthotopic implantation. Six-week-old female BALB/c nude mice were anesthetized by i.p. injection of 2.2.2-tribromoethanol (Aldrich Chemical, Milwaukee, WI, USA) at the dose of 0.28 mg/g bodyweight. Then, after making a small median abdominal incision in the mice under anesthesia, 2×10^6 cells in 0.05-mL volume of RPMI medium were inoculated into the middle wall of the greater curvature of the glandular portion of the stomach using a 30-gauge needle (Nipro, Tokyo, Japan). The stomach was then returned into the peritoneal cavity, and the abdominal wall and skin were closed with an AUTOCLIP applier (Becton-Dickinson, Sparks, MD, USA). The mice were killed 200 days after the tumor cell inoculation or when moribund, and peritoneal dissemination was evaluated by counting the number of tumor nodules in the mesenterium. The body organs were examined for metastasis, and various tissues were processed for histological examination.

Evaluation of the growth rate and metastatic potential of the cell lines. The tumorigenicity and spontaneous-metastatic potential of the cell lines were tested by s.c. injection of $0.5–1 \times 10^7$ cells suspended in 0.2 mL of RPMI1640 medium into 6-week-old female BALB/c nude mice. All the mice were numbered, housed separately, and examined twice weekly for tumor development. The tumor mass was measured in two dimensions with calipers, and the tumor volume was calculated according to the equation $(l \times w^2)/2$ (l = length, w = width). At appropriate intervals or when moribund, the mice were killed, and various organs and tissues were examined for metastasis and processed for histological examination as described.[11]

Therapeutic studies with CPT-11 and GEM. Orthotopic implantation of 2×10^6 44As3 or 58As1 cells was conducted in 6-week-old female BALB/c mice (Day 0). The experimental mice were divided into a control group that received vehicle alone (saline), and experimental groups that received i.v. inoculation of different doses of the drugs (50–200 mg/kg/mouse). On Days 3, 7 and 11, tumor-bearing mice received an i.v. injection of 7-Ethyl-10-[4-(1-piperidino)-1-piperidino] carboxycamptothecin (CPT-11). CPT-11 was purchased from Yakult Honsha (Tokyo, Japan) and dissolved in saline before being injected i.v. Gemcitabine (gemcitabine hydrochloride), chemically characterized as (+)-2′-deoxy-2′, 2′-difluorocytidine monohydrochloride, was purchased from Eli Lilly Japan (Kobe, Japan). The mice were administered i.v. inoculations of GEM on days 3, 7, 10, 14, 17, and 21. Seven mice from each group were killed when moribund, or on Day 70.

Statistical analysis. All the data were expressed as the mean ± SE, and analyzed using the unpaired t-test and a *P*-value of less than 0.001 was considered to denote statistical significance.

RT-PCR analysis. Total RNA was extracted using the ISOGEN/ISOGEN-LS Poly (A) + Isolation Pack (Nippon Gene, Tokyo, Japan), in accordance with the supplier's protocol. After reverse transcription using 1 μg total RNA with an oligo (dT) primer, the whole mixture was used for PCR detecting human and murine β actin. The primers used were as follows; human β actin forward primer, GGAAATCGTGCGTGACATT; reverse primer, CATCTGCTGGAAGGTGGACAG; murine β actin forward primer, GAAATCGTGCGTGACATCAAA; reverse primer, TACTGGTGCTAGGAGCCA. PCR was performed using an RNA PCR kit (Applied Biosystems, Foster City, CA, USA), under the following conditions; initial denaturation at 95°C for 2 min, 35 cycles of amplification (denaturation at 95°C for 60 s and annealing at 60°C for 60 s), and extension at 72°C for 7 min. The PCR products were electrophoresed on 2% agarose gel, and stained with ethidium bromide.

Gene expression profiling by cDNA microarray analysis. 5 μg total RNA was amplified using an *in vitro* transcription reaction.[15] The amplified RNA (6 μg) was reverse-transcribed using random hexamers and aminoallyl-dUTP. The synthesized cDNA was labeled by allowing it to react with a dye (NHS-ester Cy3 or Cy5, Amersham Biosciences, Buckinghamshire, UK).[16] The labeled cDNA was applied to the DNA microarray (Human IA; Agilent Technologies, Palo Alto, CA, USA) and hybridized at 65°C for 17 h. After washing, the microarray was scanned on a scanner (Agilent, G2565BA) and the image was analyzed using a Feature Extraction software (Agilent). The signal intensity of each spot was calibrated by subtraction from the intensity of the negative control. Global normalization methods were used for identification of the differentially expressed genes in each microarray experiment.

Immunohistochemical Analysis. Mouse antibodies against human Cathepsin L (C2970) and MMP-1 (M6427: Sigma-Aldrich, St. Louis, MO, USA), human VEGF (JH121: Laboratory Vision, Fremont, CA, USA), human EGER (31G7: Zymed Laboratory, San Francisco, CA, USA) and human Smad4 (B-8; Santa Cruz Biotechnology, Santa Cruz, CA, USA) were used for this study. The other antibodies used have been described in a previous study.[14] Immunohistochemical staining was carried out as described previously.[8] The staining was repeated to check for possible technical errors, but the results were consistent. Scores for the expression of various genes were assigned semiquantitatively according to the percentage of the cells stained and the staining intensity.

Results

Establishment of the highly metastatic cell lines. Following s.c. inoculation, 20–40% of the HSC-44PE and HSC-58 cells (cultured scirrhous gastric carcinoma cells) metastasized spontaneously to the regional lymph nodes and lungs. When the subclones isolated by repeated s.c. injection of these cells were implanted orthotopically, they spread to the greater omentum,

 doi: 10.1111/j.1349-7006.2005.00054.x

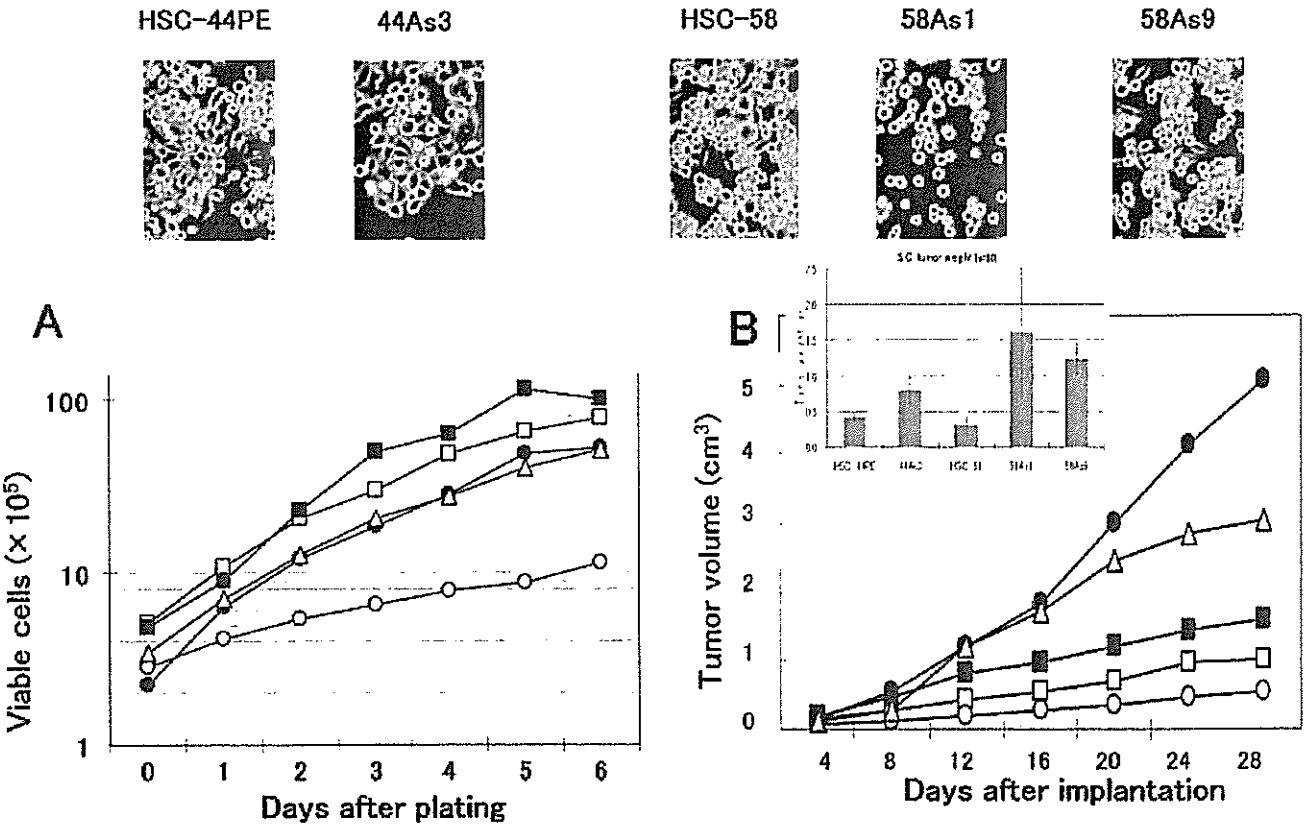

Fig. 1. Phase-contrast micrographs and the growth properties of the sublines showing a high metastatic potential and their parent cell lines. Original magnification, × 200. (A), Growth curves of the cells *in vitro*. Cells were seeded at a density of 1×10^5 cells/well in 6-well plates (Falcon, Lincoln Park, NJ, USA), and the cell numbers were determined daily. The results of a representative experiment are given and the points indicate the average of the results in 3 wells in which the cell numbers varied by 10%. (B), Growth curves of the cells *in vivo*. Tumor volume was measured at predetermined time intervals described in 'Materials and Methods.' HSC-44PE (□), 44As3 (■), HSC-58 (○), 58As1 (●), and 58As9 (△) cell lines were used. Similar results were obtained in a second experiment conducted independently.

mesenterium and so on, and caused the formation of bloody ascites in a small number of animals.[14] Following this result, we incubated the cancer cells isolated from the ascitic fluid of mice, which developed cancerous peritonitis 3–6 months following the orthotopic implantation of HSC-44PE and HSC-58 cells, and attempted orthotopic injection of the incubated cells. This sequence of manipulations was repeated for 12 cycles in an attempt to reliably isolate cell lines that would have higher potentials of undergoing metastasis (in the form of dissemination) over short periods of time. We first obtained a cell line (44As3) from HSC-44PE cells that possessed a high metastatic potential, with a strong capability of inducing ascites. The 44As3 cells resembled the parent HSC-44PE cells in their morphological characteristics. While most cells of this subline exhibited high adhesivity, a small number of spherical cells remained floating and showed proliferative activity. Occasional signet ring cells were also observed (Fig. 1). Although the proliferative potential of the 44As3 cells did not differ greatly from that of the parent cell line *in vitro* (Fig. 1A), the former induced more rapid s.c. tumor formation than the latter (Fig. 1B).

Two highly metastatic cell lines (58As1 and 58As9) were also established from the HSC-58 cells. The 58As1 cells assumed the form of aggregates of spherical cells with low adhesive capacity, which remained floating and showed proliferative activity. In contrast, 58As9 cells often exhibited high adhesivity, resembling the parent cell line, HSC-58, in this characteristic (Fig. 1). Both 58As1 and 58As9 cells exhibited higher proliferative potential *in vitro* than the parent HSC-58 cells (Fig. 1A), and the tumor-forming capability following s.c. injection of these subclones differed markedly from that of the parent cell line; the 58As1 cells, in particular, showed a markedly higher tumor-forming capability (Fig. 1B).

Comparison of the highly metastatic cell lines and the parent cell lines *in vivo*. Table 1 shows the metastatic behavior and the survival days of animals following orthotopic injection of the tumor cells. Orthotopic implantation of 44As3 cells resulted in the formation of bloody ascites approximately 20 days later, and some mice became moribund (Fig. 2D). Dissemination was most often seen to the greater omentum, mesenterium, parietal peritoneum, diaphragm, and so on. Metastasis to the regional lymph nodes and liver was also frequently seen (Table 1). Micrometastasis was observed in the pancreas (also in the lungs, although rarely). The percentage of parent HSC-44PE cells that survived at the site of implantation was 68%. Inoculation of HSC-44PE cells resulted in the animals becoming moribund approximately 85 days after the implantation, but none of the animals developed ascites (Table 1, Fig. 2D).

When 58As1 or 58As9 cells were implanted orthotopically, bloody ascites began to form approximately 3 weeks after the inoculation, accompanied by tumor dissemination to the greater omentum, mesenterium, parietal peritoneum, diaphragm and so on, and the animals died soon thereafter (Table 1, Fig. 2A–C). Lymph node metastasis was observed in all the animals; metastasis to the liver was also noted. Micrometastases were seen in the pancreas and the lungs. Implantation of 58As1 cells was followed by the development of micrometastases in the

Table 1. Metastasis and peritoneal dissemination after orthotopic inoculation of human gastric cancer cell lines and sublines[1]

Cell line	Survival days	Tumor formation	Ascites	Lymph node	Lung[2]	Liver	Pancreas[2]	Kidney[2]	Disseminated Metastasis			
									Omentum	Mesenterium	Parietal peritoneum	Diaphragm
HSC-44PE	131 ± 44 (85–200)	13/19 (68%)	0/13 (0%)	5/13	0/13	0/13	0/13	0/3	4/13	3/13	2/13	0/13
44As3	33 ± 11 (20–62)	21/21 (100%)	19/21 (90%)	21/21	2/21	19/21	10/21	0/21	21/21	21/21	20/21	14/21
HSC-58	85 ± 16 (68–123)	16/20 (80%)	1/16 (6%)	5/16	1/16	3/16	1/16	0/16	6/16	3/16	3/16	0/16
58As1	32 ± 5 (23–42)	21/21 (100%)	20/21 (95%)	21/21	6/21	19/21	7/21	4/21	21/21	21/21	21/21	13/21
58As9	45 ± 13 (22–68)	14/14 (100%)	14/14 (100%)	14/14	2/14	7/14	1/14	0/14	14/14	10/14	11/14	8/14

[1]Mice were killed at 200 days after the orthotopic implantation. Data are shown as the number of mice bearing metastasis at the site/total number of mice bearing tumor. [2]Micrometastasis.

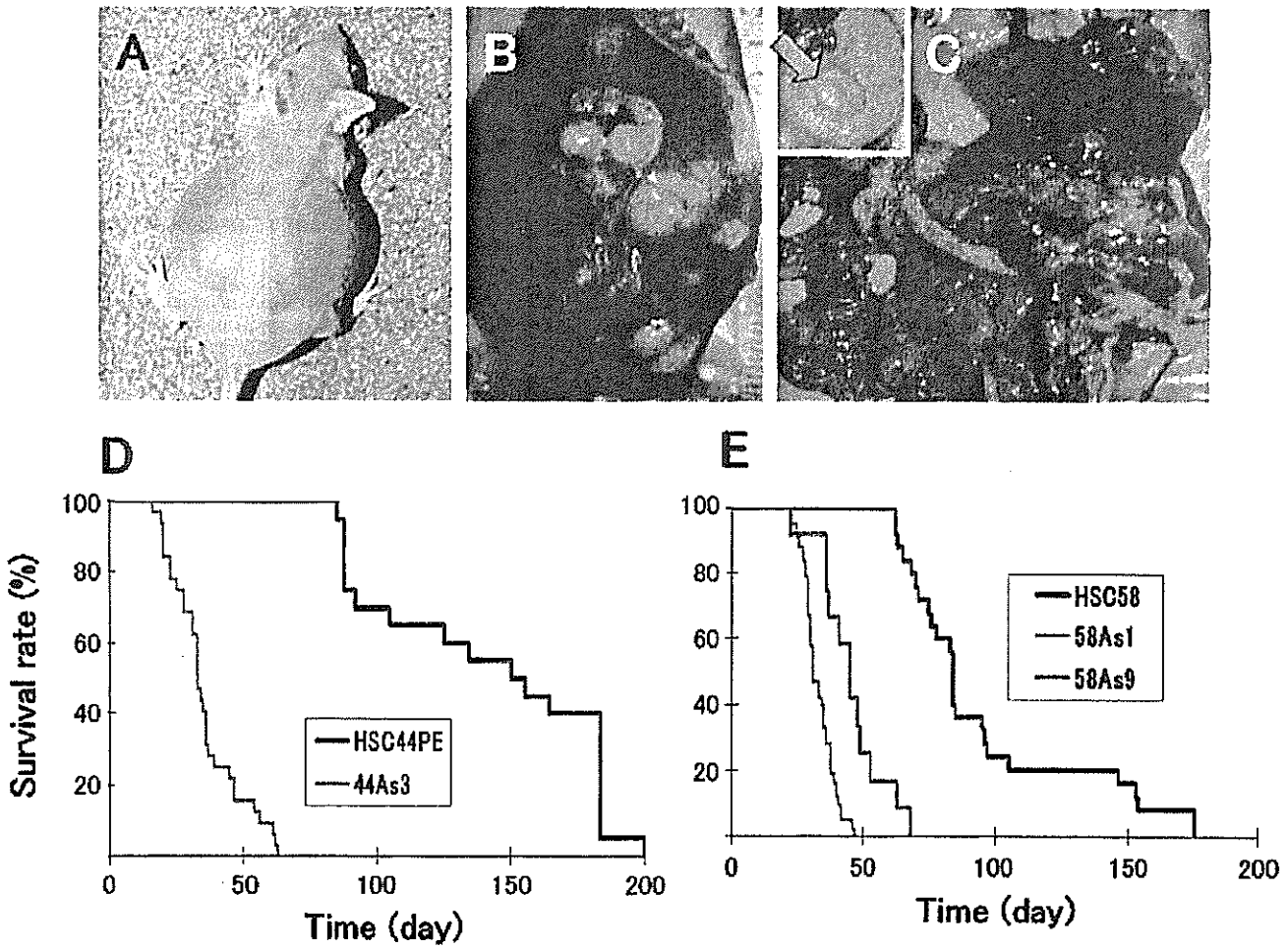

Fig. 2. Macroscopic appearance of the peritoneal disseminations, and survival of nude mice after orthotopic implantation of the cell lines. (A,B), Carcinomatous peritonitis was observed 4 weeks after orthotopic implantation of 58As1 cells. Abdominal distension because of bloody ascites was evident. (C), Peritoneal dissemination was recognized from the innumerable whitish nodules visualized in the abdominal cavity, mesenterium, omentum, parietal peritoneum and diaphragm. Orthotopic implantation of 58As1 cells in the stomach of nude mice was followed by tumor formation 3 weeks later (green arrow, inset). (D), Survival of 44As3-, and HSC-44PE-tumor-bearing mice ($n = 15$; $P < 0.001$). (E), Survival of 58As1-, 58As9-, and HSC-58-tumor-bearing mice ($n = 20$; $P < 0.001$). The experiments were repeated thrice and yielded similar results each time.

 doi: 10.1111/j.1349-7006.2005.00054.x

Table 2. Genes that show differential expression levels in 44As3 cells as compared with those in HSC-44PE cells

Ratio	Symbol	Gene name	Function and description
Upregulated gene			
29.63	*MMP1*	Matrix metalloproteinase 1	Proteolysis and peptidolysis, collagenase
11.25	*LOC57402*		Cell signaling
9.68	*I_1109564*	H19	Unknown function
4.92	*LGALS1*	Lectin, galactoside-binding, galectin 1	Apoptosis, cell adhesion
4.84	*I_930461*	Tropomyosin 2 (beta)	Contractile proteins
4.47	*AGR2*	Anterior gradient 2 homolog (Xenepus laevis)	Oncogenesis
4.40	*BOK*	BCL2-related ovarian killer	Induction of apoptosis
4.03	*NAP1L4*	Nucleosome assembly protein 1-like 4	Nucleosome assembly
3.99	*TNC*	Tenascin C (hexabrachion)	Binding, cell adhesion
3.98	*HSPB1*	Heat shock 27 kDa protein 1	Regulation of translational initiation
3.95	*HGD*	Homogentisate 1,2-dioxygenase	Tyrosine catabolism, phenylalanine catabolism
3.83	*PIGPC1*		Plasma membrane protein actvated by p53, cell death
3.52	*PIASY*		Apoptosis
3.48	*SYP*	Synaptophysin	Regulating neurotransmitter release
3.38	*RPS12*		Ribosomal protein S12
3.36	*CTSL*	Cathepsin L	Associated with highly invasive tumors
3.35	*HSPC018*		Unknown function
3.23	*INSIG1*	Insulin induced gene 1	Metabolism, cell proliferation
3.20	*I_962761*	Insulin induced gene 1	Metabolism, cell proliferation
3.17	*I_963048*		Immunity
Downregulated gene			
0.14	*THBS1*	Thrombospondin 1	Endopeptidase inhibitor, signal transducer, cell adhesion
0.34	*PRG1*	Proteoglycan 1, secretory granule	Proteoglycan
0.41	*CUL4B*	Cullin 4B	Cell cycle
0.41	*MCM3*	MCM3	Adenosinetriphosphatase, DNA binding
0.42	*NFE2L3*	Nuclear factor (erythroid-derived 2)-like 3	Transcription coactivator, transcription factor
0.43	*THBS4*	Thrombospondin 4	Heparin binding, calcium ion binding, cell adhesion
0.45	*CD59*	CD59 antigen p18–20	Lymphocyte antigen, defense response, signal transduction
0.46	*VBP1*	von Hippel-Lindau binding protein 1	Protein binding
0.46	*LOC51659*		Unkown function
0.47	*PODXL*		Lymphocyte adhesin and homing
0.47	*H2BFB*		H2B histon family member B
0.47	*ZNF195*	Zinc finger protein 195	
0.47	*MCT-1*		Cyclin, cell cycle
0.48	*CD44*	CD44 antigen	Transmembrane glycoprotein, extracellular matrix attachment
0.48	*NDUFA1*	NADH dehydrogenase (ubiquinone)	Energy pathways

kidney also. Although only rarely, pleural effusion and ovarian micrometastases were also noted (data not shown). Orthotopic injection of the parent cell line (HSC-58), however, resulted in the mice becoming moribund approximately 68 days after the implantation (Table 1, Fig. 2E). When the dead animals were autopsied, mild peritoneal dissemination was noted, but ascites were observed in only a very small number of animals (Table 1).

Comparison of gene expression between the highly metastatic- and the parent cell lines. The parent cell lines with a low potential for peritoneal dissemination were compared with the highly metastatic cell lines, using a cDNA microarray (approximately 30 000 genes; Agilent). The differences in the gene expression levels between the two types of cell lines were assessed by measuring the ratios of their expression. The ratio was rated as significant when it was over 2:1. The first 15 genes ranked in terms of this ratio are shown in Tables 2 and 3. When the highly metastatic cell line 44As3 was compared with its parent cell line HSC-44PE, the expression of 89 genes, such as that of MMP1 and cathepsin L, was more intense and that of 19 genes; for example, thrombospondin 1 was less intense in the 44As3 cells in comparison to the parent cell line (Table 2). Table 2 shows the results of a similar comparison of 58As1 and 58As9 cells (highly metastatic cell lines showing a marked increase of proliferative potential) with the parent cell line, HSC-58. Compared to that in the parent cell line, 58As1 cells showed more intense expression of 40 and less intense expression of 20 of the genes examined, while 58As9 cells showed more intense expression of 36 and less intense expression of 32 of the genes examined. In addition to the MMP1 and cathepsin L genes, genes encoding molecules associated with cell adhesion, motility, proliferation, apoptosis, metabolic enzymes and so on, also showed altered expression.

Then, the expression levels of MMP1 and cathepsin L were confirmed at the protein level and compared with the expression levels of known metastasis-associated genes (Table 4). Weak MMP1 protein expression was seen in 44As3 cells as well as 58As9 cells. The cathepsin L gene was expressed in HSC-44PE cells, but even stronger expression was observed in the 44As3 cells (Fig. 3A,B). Intense expression of this gene was also seen in the metastatic cell line, 58As1 (Fig. 3C). Moderate expression of the cathepsin L gene was observed in 58As9 cells, whereas expression of this gene was totally absent in the parent cell line (Fig. 3D). Molecules whose expression levels differed markedly between the parent cell line and the 58As1 or 58As9 cells were dysadherin, CD44, integrin β4, EGFR (Fig. 3E,F), HGF, and VEGF (Fig. 3G,H). While dysadherin was not expressed in the HSC-58 cells, it was expressed intensely in all the highly metastatic subclones (Fig. 3I,J). Intense expression of nm23

Table 3. Genes that show differential expression levels in 58As1 and 58As9 compared with that in HSC-58 cells

Ratio	Symbol	Gene name	Function and description
Upregulated genes 58As1			
19.41	*ADH1C*	Alcohol dehydrogenase 1C, gamma polypeptide	Zinc ion binding, electron transporter, metabolism
18.59	*ADH1B*	Alcohol dehydrogenase IB, beta polypeptide	Zinc ion binding, electron transporter, metabolism
17.70	*FABP1*	Fatty acid binding protein 1, liver	Lipid transporter, fatty acid metabolism, cell signaling
15.21	*ADH1A*	Alcohol dehydrogenase 1A, alpha polypeptide	Zinc ion binding, electron transporter, metabolism
14.15	*PLAT*	Plasminogen activator, tissue	Proteolysis and peptidolysis, blood coagulation
11.01	*MTP*	Microsomal triglyceride transfer protein subunit precursor	Lipid metabolism, Small molecule-binding protein
10.47	*AKR1C2*	Aldo-keto reductase family 1, member C2	Bile acid electron transporter, metabolism
4.71	*CYP1B1*	Cytochrome P450, family 1, subfamily B, polypeptide 1	Cytochrome P450, electron transporter, morphogenesis
4.67	*AKR1C3*	Aldo-keto reductase family 1, member C3	Electron transporter, metabolism, cell proliferation
4.04	*PON2*	Paraoxonase 2	Arylesterase
4.01	*RDHL*		NADP-dependent retinol dehydrogenase/reductase
3.73	*SERPINE2*	Serine proteinase inhibitor, clade E, member 2	Serpin, development
3.60	*PPP1R14A*	Protein phosphatase 1, regulatory subunit 14A	
3.54	*TGFBI*	Transforming growth factor, beta-induced, 68 kDa	Integrin binding, tumor suppressor, cell adhesion
3.45	*PROCR*	Protein C receptor, endothelial (EPCR)	Receptor, inflammatory response
Upregulated genes 58As9			
7.03	*AKR1C2*	Aldo-keto reductase family 1, member C2	Bile acid transporter, binding, electron transporter
6.08	*I_1109564*	H19, imprinted maternally expressed untranslated mRNA	Unknown function
5.95	*MKNK2*	MAP kinase-interacting serine/threonine kinase 2	Phosphorylation, signal transduction
4.10	*APOC1*	Apolipoprotein C-I	Lipid metabolism
4.07	*FLJ21841*		Unknown function
4.02	*SERPINE2*	Serine proteinase inhibitor, clade E, member 2	Serpin, development
3.77	*CTSL*	Cathepsin L	Cathepsin L, associated with highly invasive tumors
3.28	*AKR1C3*	Aldo-keto reductase family 1, member C3	Electron transporter, metabolism, cell proliferation
3.11	*SIAT8B*	Sialyltransferase 8B (alpha-2, 8-sialyltransferase)	Metabolism, embryogenesis and morphogenesis
3.01	*FKBP1B*	FK506 binding protein 1B	Popeptidylprolyl isomerase
2.82	*KIAA1247*		Member of the sulftase family
2.80	*I_1000731*	GRB2-associated binding protein 2	Protein-protein and protein–lipid interactions
2.77	*STMN3*	Stathmin-like 3	Neurogenesis, SCG10 like-protein, tumor progression
2.75	*ANK3*	Ankyrin 3, node of Ranvier (ankyrin G)	Cytoskeletal anchoring, vesicle transport
2.74	*CEBPE*	CCAAT/enhancer binding protein (C/EBP), epsilon	Transcription activating factor, defense response
Downregulation 58As1			
0.11	*LAMR1*	Laminin receptor 1	Signal transduction, cell adhesion, invasive growth
0.13	*S100A4*	S100 calcium binding protein A4	Calcium ion binding, invasive growth
0.15	*RARRES1*	Retinoic acid receptor responder	Negative regulation of cell proliferation
0.15	*HLA-DQB1*	HLA complex, class II, DQ beta 1 precursor	Immune response
0.15	*KLK6*	Kallikrein 6 (neurosin, zyme)	Serine-type peptidase, pathogenesis
0.16	*TM4SF4*	Transmembrane 4 superfamily member 4	Negative regulation of cell proliferation, glycosylation
0.16	*HLA-DRA*	Major histocompatibility complex, class II, DR alpha	Immune response
0.17	*CTNNB1*	Catenin (cadherin-associated pritein), beta 1, 88 kDa	Tumor suppressor, cell adhesion, transcription
0.19	*HLA-DRB3*	Major histocompatibility complex, class II, DR beta 3	Immune response
0.20	*SAT*	Spermidine/spermine N1-acetyltransferase	Diamine N-acetyltransferase, modulates tumorigenicity
0.20	*HLA-DRB5*	Major histocompatibility complex, class II, DR beta 5	Immune response
0.20	*I_966873*		Strong similarity to human HLA-DRB1
0.21	*FOS*	v-fos FBJ murine osteosarcoma viral oncogene homolog	Transcription, methylation, cell growth, oncogenesis
0.21	*I_965396*		Unknown, high similarity to charcterized human AG2
0.22	*CEACAM6*	Carcinoembryonic antigen-related cell adhesion molecule 6	Signal transduction, cell-cell signaling
Downregulation 58As9			
0.06	*CEACAM8*	Carcinoembryonic antigen-related cell adhesion molecule 8	Tumor antigen, immune response, cell adhesion
0.07	*TM4SF3*	Transmembrane 4 superfamily member 3	Signal transducer, tumor antigen, pathogenesis
0.07	*LAMR1*	Laminin receptor 1 (ribosomal protein SA, 67 kDa)	Signal transduction, cell adhesion, invasive growth
0.09	*CEACAM6*	Carcinoembryonic antigen-related cell adhesion molecule 6	Signal transduction, cell-cell signaling, cell adhesion
0.12	*CTNNB1*	Catenin (cadherin-associated pritein), beta 1, 88 kDa	Tumor suppressor, cell adhesion, oncogenesis
0.12	*KRT19*	Keratin 19	Structural constituent of cytoskeleton, differentiation
0.13	*KRTHA3A*	Keratin, hair, acidic, 3 A	Cell shape and cell size control
0.13	*CEACAM3*	Carcinoembryonic antigen-related cell adhesion molecule 3	Tumor antigen, immune response, cell adhesion
0.14	*I_966690*		Strong similarity to human HLA-DRB4
0.17	*S100A4*	S100 calcium binding protein A4	Calcium ion binding, invasive growth
0.20	*FOS*	v-fos FBJ murine osteosarcoma viral oncogene homolog	Transcription, methylation, cell growth, oncogenesis
0.22	*DAF*	Decay accelerating factor for complement (CD55)	Decay accelerating factor
0.23	*MYC*	v-myc myelocytomatosis viral oncogene homolog (avian)	Transcription factor, cell cycle, pathogenesis
0.24	*CRIP1*	Cysteine-rich protein 1 (intestinal)	Zinc ion binding, cell proliferation
0.24	*KRTHB6*	Keratin, hair, basic, 6	Monilethrix

 doi: 10.1111/j.1349-7006.2005.00054.x

Table 4. Expression of metastasis-related genes in the highly metastatic and the parent gastric cancer cell lines

Cell line	MMP-1	Cathepsin L	Cell adhesion					Oncogenes					Angiogenesis				nm23	Smad4
			CD44	E-cadherin	Dysadherin	β-catenin	Integrin α6β4	EGFR	c-erb-B-2	cript	c-met	HGF	bFGF	VEGF	IL-6	IL-8		
44As3	+	++	++a	++	++	++	—	++	−	+	+	−	−	+	−	−	++	−
HSC-44PE	−	+	++a	++	++	++	−++	++	−	+	+	+	−	+	−	−	−	−
58As1	−	++	++	−	++	++	−++	+	−	+	++a	++	+	++	−	−	++	−
58As9	+	+	++	−	++	+	−+	++	−	+	++a	+	+	++	−	−	+	−
HSC-58	−	−	+	−	−	++	—	−	−	+	++a	−	+	−	−	−	−	−

Immunohistochemical staining was carried out as described in a previous study.[6] ++, Moderate or strong staining intensity, or staining of > 75% of the cells; +, weak staining intensity, or staining of < 25% of the cells; −, negative staining, or staining of < 1% of the cells. a, gene amplification.

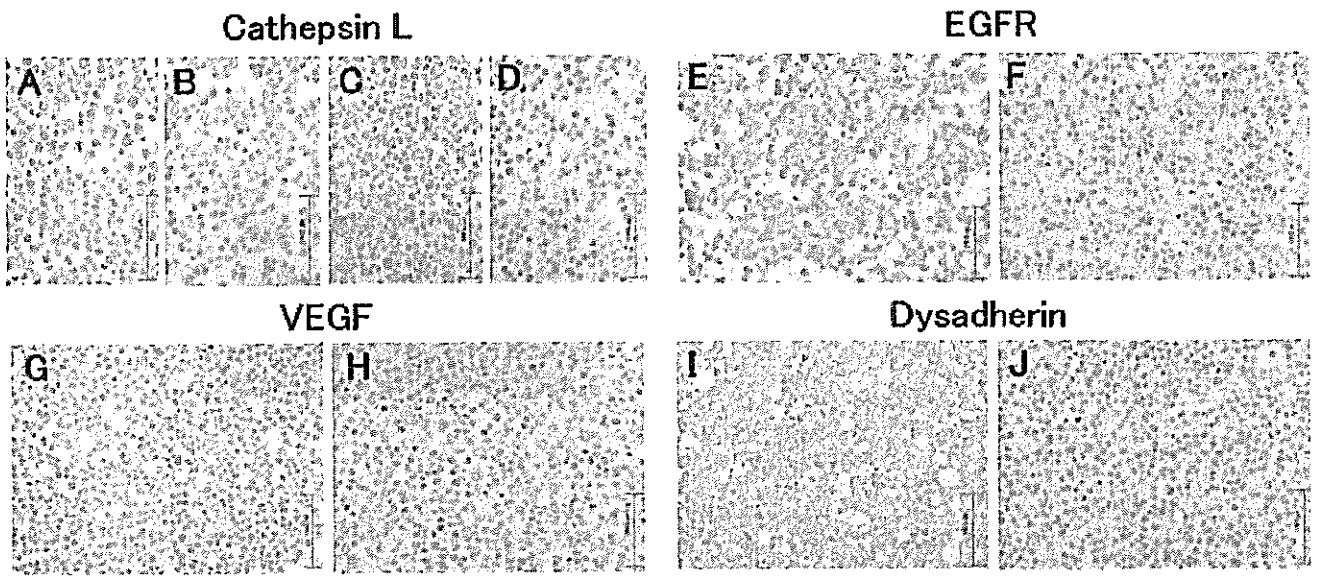

Fig. 3. Immunohistochemical analyses of Cathepsin L, EGFR, VEGF and Dysadherin in the highly metastatic and the parent cell lines. The metastatic 44As3 (A) and 58As1 (C) expressed strongly detectable cathepsin L in the cytoplasm. Immunoreactivity for cathepsin L observed weakly at the cytoplasm in HSC-44PE (B), but immunoreactivity completely absent from HSC-58 (D). (E), Expression of EGER is observed in the membranes of the 58As1 subclone. (F), Immunoreactivity for EGER was completely absent from HSC-58 cells. (G), Expression of VEGF is observed in the cytoplasm of the 58As9 cells, but immunoreactivity absent from HSC-58 (H). (I), Expression of dysadherin is observed at the cell-cell boundaries in 58As9 subclone. (J), Immunoreactivity for dysadherin was completely absent from HSC-58 cells.

was also observed in highly metastatic cell lines, while Smad4 expression was not seen in these cell lines.

Usefulness of the model as a tumor metastasis model for the evaluation of drugs. All of the highly metastatic cell lines served as highly reproducible models of peritoneal dissemination, and a quantitative relationship was observed between the number of inoculated cells and the animal survival rate (incidence of tumor) (data not shown). Next we evaluated antitumor effects of antitumor agents in this model. We selected CPT-11[17] and GEM[18] as representative cytotoxic agents. Figure 4A shows the survival curve of the 58As1 implanted mice treated with CPT-11. Most of the animals belonging to the untreated control group died of extensive peritoneal dissemination approximately 30 days after the implantation. In the CPT-11-treated group (200 mg/kg/head), however, 60 days passed before the first animal death was noted. Thus, treatment with CPT-11 significantly ($P < 0.001$, unpaired t-test) prolonged the survival of the animals injected with the tumor cells, and dose-dependency was evident when the data from multiple groups were compared. Similar results were also obtained for 44As3 cells (Fig. 4B). Figure 4(C) shows the results of the experiment in which GEM was administered intravenously following orthotopic inoculation of 58As1 cells. The survival period was significantly prolonged in the GEM-treated group (100 mg/kg/head). Similar results were also obtained for mice implanted with the 44As3 cells (data not shown).

To identify the stage of tumor metastasis suppressed by these agents, RT-PCR analysis was performed with sets of primers specific for human and mouse β actin, respectively. Cells collected from the intraperitoneal lavage fluid 21 days after orthotopic implantation of 58As1 cells served as the samples. Autopsy examination revealed that there was no macroscopic tumor formation in the gastric wall of the drug-treated animals, while peritoneal dissemination was noted in the untreated control group. Figure 4(D) shows two typical animals used for each experimental group. In the untreated control group, RT-PCR product represents human-derived β actin gene was clearly identified (lanes 3 and 4). In the CPT-11- and GEM-treated groups, however, the gene sequence of human origin was less clear (lanes 5, 6 and 7, 8, respectively). These results suggested that

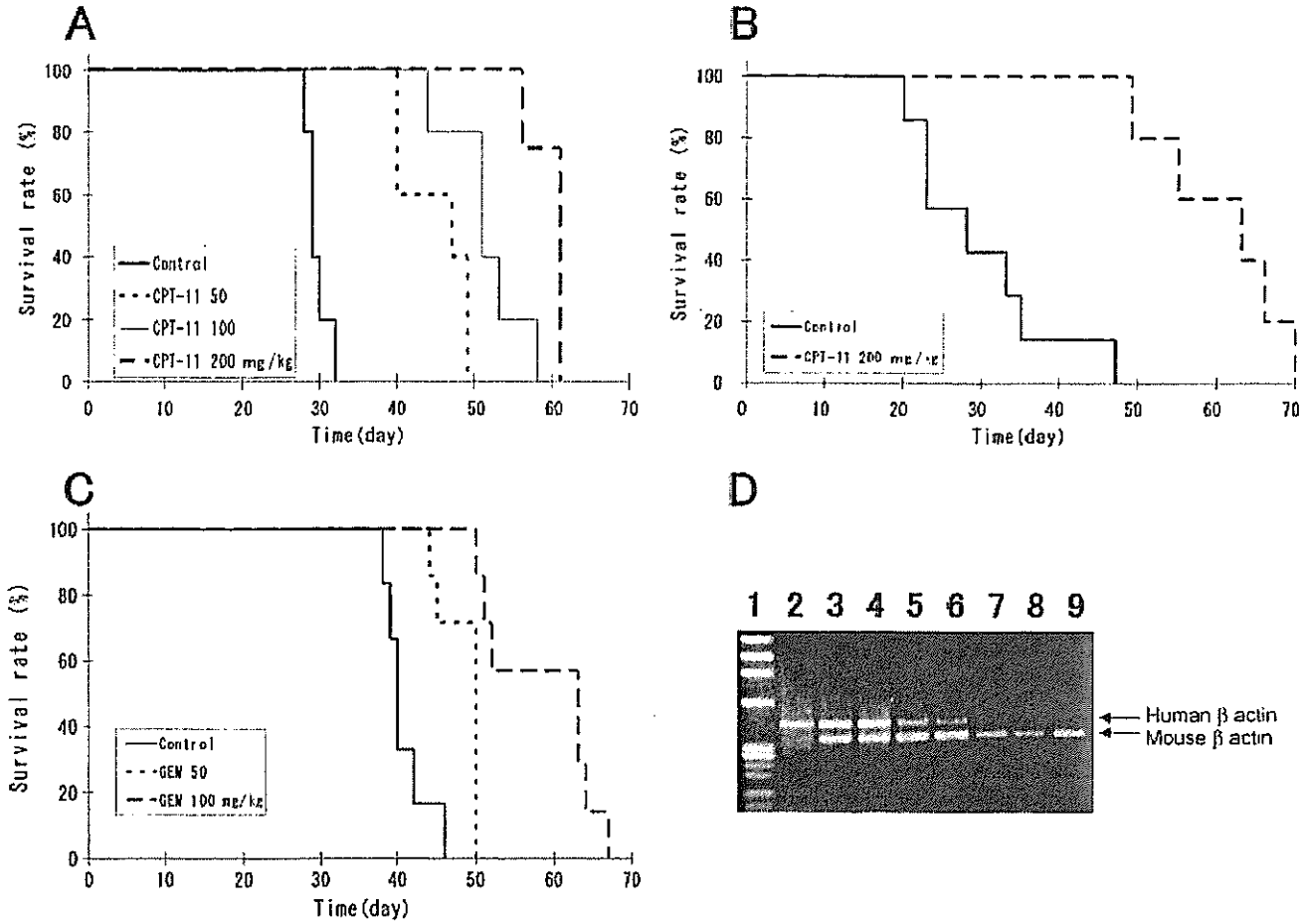

Fig. 4. Effects of CPT-11 and GEM in the peritoneal dissemination mouse model established using orthotopically implanted 44As3 or 58As1 cells. Mice receiving CPT-11 or GEM, or vehicle alone as control, were monitored daily for the development of peritoneal dissemination. (A), Survival of 58As1-tumor-bearing mice after CPT-11 treatment ($n = 5$; $P < 0.001$). This experiment was repeated thrice and similar results were observed each time. (B), Survival of 44As3-tumor-bearing mice after CPT-11 treatment ($n = 6$; $P < 0.001$). (C), Survival of 58As1-tumor-bearing mice after GEM treatment ($n = 7$; $P < 0.001$). Similar results were obtained in two independent experiments. (D), CPT-11 and GEM inhibit dissemination of cancer cells into the peritoneal cavity *in vivo*. RT-PCR was performed on the disseminated cells isolated from the intraperitoneal lavage fluid (2 mL of PBS) using human-specific and mouse-specific primers against β-actin. The total amount of RNA (200 ng) was equalized in all the samples. Lane 1, maker; lane 2, human gastric cell line HSC-39; lanes 3 and 4, untreated control group; lanes 5 and 6, 200 mg/kg CPT-11-treated group; lanes 7 and 8, 100 mg/kg GEM-treated group; lane 9, murine leukemia cell line P388.

treatment with the agents reduced the number of cancer cells in the peritoneal cavity. It was also found that the drugs directly inhibited the growth of s.c. tumors following implantation of 58As1 and 44As3 cells (data not shown). From these results, it is considered highly likely that while the agents suppress metastasis of these tumor cells by suppressing tumor formation at the implanted site, the small number of tumor cells remaining within the peritoneal cavity gradually proliferate, making it difficult to obtain better therapeutic results than some prolongation of the survival period.

Discussion

In the present study, we isolated 44As3 cells from HSC-44PE, and 58As1 and 58As9 cells from HSC-58, and succeeded, in a reliable manner, in establishing a model in which peritoneal dissemination occurred from a primary lesion of gastric carcinoma. The 44As3, 58As1 and 58As9 sublines were generated by the conventional method, that is by selection of highly metastatic clones (found in small numbers among cancer cells showing poor metastatic potential) *in vivo*.[19] On the basis of a study using clinical samples for microarray analysis of primary and metastatic lesions, investigators recently suggested that primary cancers with a high metastatic potential may differ in nature from those having a poor metastatic potential.[20] However, the results of our study support the conventional view that clones with a high metastatic potential contained in small amounts among the cancer tissues are responsible for the formation of metastatic lesions.

We consider that the establishment of this model is significant in the following respects: (i) it allows reproduction of all the steps in the development of cancerous peritonitis, from the stage of infiltrative growth of the tumor within the gastric mucosa to peritoneal dissemination and formation of ascites; (ii) it is an animal model of metastatic gastric cancer that closely resembles that in clinical cases; (iii) quantitative analysis is possible with this model, because it is established from cultured cells. The model is expected to be useful for the study of the continuity or association between infiltrative growth/peritoneal dissemination and gene expression, mechanism of formation of bloody ascites, and analysis of the microenvironmental factors influencing the development of the metastases. Comparison of the expression

 doi: 10.1111/j.1349-7006.2005.00054.x

levels of the relevant genes among different cell lines with markedly varying metastatic potential may be expected to allow isolation of new molecules involved in the peritoneal dissemination of tumors. Furthermore, these sublines are also expected to contribute to advancement of the functional analysis of the involvement of the newly identified molecules in peritoneal dissemination.

Following recent advances in the comprehensive analysis of gene expression, it has been gradually revealed that gene expression patterns undergo complex alterations during the course of metastasis of gastric carcinoma.[21–27] cDNA array analysis carried out using cell lines with varying metastatic potentials in the present study revealed altered expressions of numerous genes in these cells, including those involved in adhesion, proliferation and metabolism. Among others, markedly increased expression of the MMP1 gene[27,28] was observed in 44As3 cells; however, the expression of MMP1 at the protein level was low in these cells, suggesting that MMP1 may not be closely involved in metastasis. Cathepsin L, involved in the degradation of the extracellular matrix,[29] was intensely expressed in not only 44As3, but also 58As1 cells. This finding was confirmed by immunostaining. Intense cathepsin L expression was also seen in 58As9 cells. These results suggest that this molecule may be closely associated with the metastatic potential of these tumor cells. Meanwhile, it is known that invasion and metastasis of gastric cancer occur as a result of accumulation of changes in several genes.[21] These include genes encoding cell adhesion-related molecules (E-cadherin,[30,31] β-catenin,[30] integrin α6β4,[6] dysadherin,[32] CD44,[33,34] etc.), molecules associated with proliferation, loss of intercellular adhesion and matrix degradation (EGF, c-erbB-2,[35] cript,[36] etc.), motility-associated molecules (HGF, c-met,[37] etc.), molecules associated with vascularization (VEGF,[38] IL-6,[39] IL-8,[40] bFGF,[41] etc.), a tumor metastasis suppressor gene (nm23)[42] a gene associated with the malignant course of tumors (Smad),[43] and so on. When the expression of these genes was analyzed, markedly increased expression of MMP1, cathepsin L and nm23 was observed in the highly metastatic 44As3 cell line as compared with that in the poorly metastatic parent cell line. Molecules expressed specifically in the highly metastatic cell lines 58As1 and 58As9 included cathepsin L, dysadherin, CD44, integrin β4, EGFR, HGF and VEGF. Although these molecules seemed to be closely related to peritoneal dissemination of gastric carcinoma, it would be desirable to determine the exact causal relationship between these molecules and tumor metastasis using *in vivo* models. Nonetheless, our results suggest that: (i) there may be multiple pathways involving different molecules for the apparently single process of tumor metastasis, and (ii) the genes contributing to the metastatic potential of tumor cells may differ between the parent cells and the clones selectively isolated from it.

As stated, the presence of peritoneal metastasis represents an advanced stage of cancer associated with a poor prognosis, and no effective therapy for this condition is available as yet. It is therefore important to devise a new therapeutic strategy based on the aforementioned novel viewpoints. One such strategy that has been discussed is the development of anticancer agents based on molecular targeting. To seek such agents, a model allowing appropriate evaluation of drugs is essential, and models to be used for drug evaluation *in vivo* need to satisfy the following six requirements: (i) the tumor should undergo proliferation, spread, dissemination and metastasis akin to those seen in clinical cases; (ii) the tumor cell survival rate in the gastric wall following orthotopic implantation should be 100%; (iii) the frequency of metastasis should be 90–100%; (iv) the model should be highly reproducible; (v) the interindividual variance should be small, to allow easy comparison among different test groups; (vi) application to experiments using many animals should be relatively easy. When the animal model of peritoneal dissemination established in this study was evaluated according to these criteria, all the three highly metastatic cell lines established satisfied all of these six requirements. We evaluated the antitumor activities of two antitumor agents (CPT-11[17] and GEM[18]) using the animal models implanted with 58As1 and 44As3 cells. Treatment with these agents suppressed the proliferation and spread of the tumor and significantly prolonged the survival of the animals. For each of the cases studied, a dose-response relationship was observed, and the experiments were highly reproducible. Another advantage of this animal model is that the length of time from implantation to tumor formation is short (causing death within 40 days); this feature may be expected to contribute to shortening of the evaluation period. The advantages of this model may prove to be useful for the development of drugs based on molecular targeting.

In the past, no approach was known for isolation of host factors involved in the cascade of tumor proliferation in the primary lesion to formation of ascites, or for the functional analysis of this cascade (e.g. analysis of interactions). The model established in the present study is expected to contribute greatly to the advancement of studies in these fields and in other applied research.

Acknowledgments

We are grateful to Dr A. Ochiai (Pathology Division, National Cancer Center Research Institute East) for fruitful discussions. This study was supported in part by a Grant-in-Aid for Cancer Research from the Ministry of Health, Labor and Welfare of Japan.

References

1 Japanese Gastric Cancer Association. Japanese Classification of Gastric Carcinoma – 2nd English Edition. *Gastric Cancer* 1998; 1: 10–24.
2 Tahara E. Endocrine tumors of the gastrointestinal tract: classification, function and biological behavior. In: Watanabe S, Wolff M, Sommers SC, eds. *Digestive Disease Pathology*. Philadelphia: Field andWood, 1988; 121–47.
3 Fenoglio-preier C, Carneiro F, Correa P *et al.* Gastric carcinoma. In: Hamilton SR, Aaltonen LA, eds. *World Health Organization Classification of Tumours. Pathology and Genetics of Tumours of the Digestive System*. Lyon: IARC Press, 2000: 37–52.
4 Maruyama K. Results of surgery correlated with staging. In: Preece PE, Cuschieri A, Wellwood JM, eds. *Cancer of the Stomach*. Orlando: Grune and Stratton, 1986; 145–63.
5 Moriguchi S, Maehara Y, Korenaga D, Sugimachi K, Nose Y. Risk factors which predict pattern of recurrence after curative surgery for patients with advanced gastric cancer. *Surg Oncol* 1992; 1: 341–6.
6 Yashiro M, Chung YS, Nishimura S, Inoue T, Sowa M. Peritoneal metastatic model for human scirrhous gastric carcinoma in nude mice. *Clin Exp Metastasis* 1996; 14: 43–54.
7 Fujita S, Suzuki H, Kinoshita M, Hirohashi S. Inhibition of cell attachment, invasion and metastasis of human carcinoma cells by anti-integrin β1 subunit antibody. *Jpn J Cancer Res* 1992; 83: 1317–26.
8 Ishii Y, Ochiai A, Yamada T *et al.* Integrin α6β4 as a suppressor and a predictive marker for peritoneal dissemination in human gastric cancer. *Gastroenterology* 2000; 118: 497–506.
9 Kotanagi H, Saito Y, Shinozawa N, Koyama K. Establishment of a human cancer cell line with high potential for peritoneal dissemination. *J Gastroenterol* 1995; 30: 437–8.
10 Kaneko K, Yano M, Tsujinaka T *et al.* Establishment of a visible peritoneal micrometastatic model from a gastric adenocarcinoma cell line by green fluorescent protein. *Int J Oncol* 2000; 16: 893–8.
11 Yanagihara K, Seyama T, Tsumuraya M, Kamada N, Yokoro K. Establishment and characterization of human signet ring cell gastric carcinoma cell lines with amplification of the c-myc oncogene. *Cancer Res* 1991; 51: 381–6.
12 Yanagihara K, Kamada N, Tsumuraya M, Amano F. Establishment and characterization of a human gastric scirrhous carcinoma cell line in serum-free chemically defined medium. *Int J Cancer* 1993; 54: 200–7.
13 Yanagihara K, Ito A, Toge T, Numoto M. Antiproliferative effects of

isoflavones on human cancer cell lines established from the gastrointestinal tract. *Cancer Res* 1993; 53: 5815–21.
14 Yanagihara K, Tanaka H, Takigahira M *et al.* Establishment of two cell lines from human gastric scirrhous carcinoma that possess the potential to metastasize spontaneously in nude mice. *Cancer Sci* 2004; 95: 575–82.
15 Luo L, Salunga RC, Guo H *et al.* Gene expression profiles of laser-captured adjacent neuronal subtypes. *Nat Med* 1999; 5: 117–22.
16 Hughes TR, Mao M, Jones AR *et al.* Expression profiling using microarrays fabricated by an ink-jet oligonucleotide synthesizer. *Nat Biotechnol* 2001; 19: 342–7.
17 Kanzawa F, Saijo N. *In vitro* interaction between gemcitabine and other anticancer drugs using a novel three-dimensional model. *Semin Oncol* 1997; 24: S7-8–S7-16.
18 Saijo N. Preclinical and clinical trials of topoisomerase inhibitors. *Ann N Y Acad Sci* 2000; 922: 92–9.
19 Fidler IJ. Rationale and methods for the use of nude mice to study the biology and therapy of human cancer metastasis. *Cancer Metast Rev* 1986; 5: 29–49.
20 Ramaswamy S, Ross KN, Lander ES, Golub TR. A molecular signature of metastasis in primary solid tumors. *Nat Genet* 2003; 33: 49–54.
21 Yokozaki H, Yasui W, Tahara E. Genetic and epigenetic changes in stomach cancer. *Int Rev Cytol* 2001; 204: 49–95.
22 Yasui W, Oue N, Ito R, Kuraoka K, Nakayama H. Search for new biomarkers of gastric cancer through serial analysis of gene expression and its clinical implications. *Cancer Sci* 2004; 95: 385–92.
23 Hippo Y, Yashiro M, Ishii M *et al.* Differential gene expression profiles of scirrhous gastric cancer cells with high metastatic potential to peritoneum or lymph nodes. *Cancer Res* 2001; 61: 889–95.
24 Hippo Y, Taniguchi H, Tsutsumi S *et al.* Global gene expression analysis of gastric cancer by oligonucleotide microarrays. *Cancer Res* 2002; 62: 233–40.
25 Hasegawa S, Furukawa Y, Li M *et al.* Genome-wide analysis of gene expression in intestinal-type gastric cancers using a complementary DNA microarray representing 23 040 genes. *Cancer Res* 2002; 62: 7012–7.
26 Weiss MM, Kuipers EJ, Postma C *et al.* Genomic profiling of gastric cancer predicts lymph node status and survival. *Oncogene* 2003; 22: 1872–9.
27 Inoue T, Yashiro M, Nishimura S *et al.* Matrix metalloproteinase-1 expression is a prognostic factor for patients with advanced gastric cancer. *Int J Mol Med* 1999; 4: 73–7.
28 Sakurai Y, Otani Y, Kameyama K *et al.* Therole of stromal cells in the expression of interstitial collagenase (matrix metalloproteinase-1) in the invasion of gastric cancer. *J Surg Oncol* 1997; 66: 168–72.
29 Dohchin A, Suzuki JI, Seki H, Masutani M, Shiroto H, Kawakami Y. Immunostained cathepsins B and L correlate with depth of invasion and different metastatic pathways in early stage gastric carcinoma. *Cancer* 2000; 89: 482–7.
30 Hirohashi S. Inactivation of the E-cadherin-mediated cell adhesion system in human cancers. *Am J Pathol* 1998; 153: 333–9.
31 Behrens J, Mareel MM, Van Roy FM, Birchmeier W. Dissecting tumor cell invasion: epithelial cells acquire invasive; properties after the loss of uvomorulin-mediated cell-cell adhesion. *J Cell Biol* 1989; 108: 2435–47.
32 Ino Y, Gotoh M, Sakamoto M, Tsukagoshi K, Hirohashi S. Dysadherin, a cancer-associated cell membrane glycoprotein, down-regulated E-cadherin and promotes metastasis. *Proc Natl Acad Sci USA* 2002; 99: 365–70.
33 Yokozaki H, Ito R, Nakayama H, Kuniyasu H, Taniyama K, Tahara E. Expression of CD44 abnormal transcripts in human gastric carcinomas. *Cancer Lett* 1994; 83: 229–34.
34 Nishimura S, Chung YS, Yashiro M, Inoue T, Sowa M. CD44H plays an important role in peritoneal dissemination of scirrhous gastric cancer cells. *Jpn J Cancer Res* 1996; 87: 1235–44.
35 Tsugawa K, Yonemura Y, Hirono Y *et al.* Amplification of the c-met, c-erbB-2 and epidermal growth factor receptor gene in human gastric cancers: correlation to clinical features. *Oncology* 1998; 55: 475–81.
36 Kuniyasu H, Yoshida K, Yokozaki H *et al.* Expression of cript, a novel gene of the epidermal growth factor family, in human gastrointestinal carcinomas. *Jpn J Cancer Res* 1991; 82: 969–73.
37 Kuniyasu H, Yasui W, Yokozaki H, Kitadai Y, Tahara E. Aberrant expression of c-met mRNA in human gastric carcinomas. *Int J Cancer* 1993; 55: 72–5.
38 Takahashi Y, Cleary KR, Mai M, Kitadai Y, Bucana CD, Ellis LM. Significance of vessel count and vascular endothelial growth factor and its receptor (KDR) in intestinal-type gastric cancer. *Clin Cancer Res* 1986; 2: 1679–84.
39 Huang SP, Wu MS, Wang HP, Yang PS, Kuo ML, Lin JT. Correlation between serum levels of interleukin-6 and vascular endothelial growth factor in gastric carcinoma. *J Gastroenterol Hepatol* 2002; 17: 1165–9.
40 Kitadai Y, Haruma K, Sumii K *et al.* Regulation of angiogenesis in human gastric carcinomas by interleukin-8. *Am J Pathol* 1998; 152: 93–100.
41 Ueki T, Koji T, Tamiya S, Nakane PK, Tsuneyoshi M. Expression of basic fibroblast growth factor and fibroblast growth factor in advanced gastric carcinoma. *J Pathol* 1995; 177: 353–61.
42 Nakayama H, Yasui W, Yokozaki H, Tahara E. Reduced expression of nm23 is associated with metastasis of human gastric carcinomas. *Jpn J Cancer Res* 1993; 84: 184–90.
43 Ijichi H, Ikenoue T, Kato N *et al.* Systemic analysis of the TGF-beta-smad signaling pathway in gastrointestinal cancer cells. *Biochem Biophys Res Commun* 2001; 289: 350–7.

 doi: 10.1111/j.1349-7006.2005.00054.x

British Journal of Cancer (2005) 92, 1877–1880
© 2005 Cancer Research UK All rights reserved 0007–0920/05 $30.00
www.bjcancer.com

Gefitinib treatment affects androgen levels in non-small-cell lung cancer patients

M Nishio*,[1], F Ohyanagi[1], A Horiike[1], Y Ishikawa[3], Y Satoh[2], S Okumura[2], K Nakagawa[2], K Nishio[4] and T Horai[1]

[1]*Division of Internal Medicine, Cancer Institute Hospital, Japanese Foundation For Cancer Research, Ariake 3-10-6, Koto-ku, Tokyo 135-8550, Japan.* [2]*Department of Chest Surgery, Cancer Institute Hospital, Japanese Foundation For Cancer Research, Tokyo, Japan.* [3]*Department of Pathology Cancer Institute, Japanese Foundation For Cancer Research, Tokyo, Japan.* [4]*Pharmacology Division, National Cancer Center Research Institute, Tokyo, Japan*

Gefitinib, an inhibitor of the epidermal growth factor receptor (EGFR, HER1/ErbB1) tyrosine kinase, has been shown to have clinical activity against non-small-cell lung cancers (NSCLCs), especially in women nonsmokers with adenocarcinomas. The aim of the present study was to clarify the relationship between androgen levels and gefitinib treatment in patients with advanced NSCLCs. Sera from 67 cases (36 men and 31 women) were obtained pretreatment and during treatment with gefitinib monotherapy (days 14–18) for examination of testosterone, dehydroepiandrosterone sulphate (DHEA), and dehydroepiandrosterone sulphate (DHEAS) levels. Testosterone and DHEA during treatment were significantly lower than the pretreatment values in both women and men, and the DHEAS levels during treatment were also significantly lowered in women. Gefitinib treatment significantly suppressed androgen levels, especially in women who had no smoking history. In addition, hormone levels in women responding to gefitinib were significantly lower during the treatment than in women who did not respond. Gefitinib-associated decrease in serum androgen levels may play a role in its clinical efficacy.

British Journal of Cancer (2005) **92,** 1877–1880 doi:10.1038/sj.bjc.6602585 www.bjcancer.com
Published online 3 May 2005

Keywords: sex hormone; epidermal growth factor receptor; tyrosine kinase inhibitor

Non-small-cell lung cancer (NSCLC) is a major health problem worldwide for both men and women (Ferlay *et al*, 2001). Usually at the time of diagnosis more than 50% of the patients have advanced or metastatic disease. While cytotoxic chemotherapy slightly prolongs survival among advanced NSCLC patients, it exerts clinically significant adverse effects (Non-Small-Cell Lung Cancer Collaborative Group, 1995; Schiller *et al*, 2002). An effective, palliative, low-toxicity treatment for patients with advanced NSCLC is therefore needed and for this purpose the epidermal growth factor receptor (EGFR/HER1) is a promising target. Gefitinib (ZD 1839, Iressa; AstraZeneca, London, UK) is an orally active, selective HER1-tyrosine kinase inhibitor (Wakeling *et al*, 2002), which has been shown to elicit objective responses in NSCLC cases, particularly in women nonsmokers with adenocarcinomas (Fukuoka *et al*, 2003; Kris *et al*, 2003). Recently, active mutations of EGFR have been identified in such cases (Paez *et al*, 2004; Pao *et al*, 2004) and may be linked with the sensitivity to gefitinib (Lynch *et al*, 2004; Paez *et al*, 2004; Pao *et al*, 2004). However, the reason why mutations frequently occur in these particular individuals is poorly understood.

Androgens are important hormones that play definitive roles in the differentiation of males and females. They can modify the activity of the epidermal growth factor network and EGFR signaling is essential for androgen-induced proliferation (Klein and Nielsen, 1993; Dammann *et al*, 2000; Torring *et al*, 2003). A receptor for androgens has been reported to occur in NSCLCs (Beattie *et al*, 1985; Kaiser *et al*, 1996) and there may be cooperative interaction between the hormones and active mutations of EGFR during the development of lung cancer. Previous reports have suggested that smoking increases the levels of androgens in men and women (Law *et al*, 1997; Trummer *et al*, 2002) and carcinogens from cigarette smoke may disrupt androgen function by reducing androgen receptor (AR) levels in androgen-responsive organs (Lin *et al*, 2004).

On the basis of these reports, we hypothesised that androgens may play an important role in the efficacy of gefitinib in NSCLC cases. In the present study, we therefore evaluated androgen levels in patients treated with gefitinib and the relationship with clinical efficacy.

PATIENTS AND METHODS

Between September 2002 and May 2004, 67 advanced or recurrent NSCLC patients were analysed in this study. All 67 were treated at our institution with gefitinib monotherapy (250 mg oral doses of gefitinib once daily) until disease progression occurred. Response evaluation and confirmation were performed in accordance with the WHO criteria (WHO, 1979). In brief, complete response (CR) was defined as complete disappearance of all lesions in imaging studies for at least 4 weeks without the appearance of any new lesions. Partial response (PR) was defined as a $\geq$50% decrease under the baseline in the sum of the products of the

*Correspondence: Dr M Nishio; E-mail: mnishio@jfcr.or.jp
Received 13 December 2004; revised 21 March 2005; accepted 21 March 2005; published online 3 May 2005

perpendicular diameters of all measurable lesions and at least stabilisation of all nonmeasurable lesions over a minimum period of 4 weeks. Progressive disease (PD) was defined as a >25% increase in the sum of the products of all measurable lesions, an unequivocal increase of nonmeasurable disease, or the appearance of new lesions. Cases were classified as having stable disease (SD) if none of the criteria for classifying responses as a CR, PR, or PD were met.

Blood was drawn before and during gefitinib administration. A previous report indicated the median time to symptom improvement with gefitinib to be only 8 days (Fukuoka *et al*, 2003), and we therefore checked the hormone levels at days 14–18, when serum was sampled between 10:00 and 14:00 and stored at 80°C for subsequent analyses. Serum levels of testosterone, dehydroepiandrosterone (DHEA), and dehydroepiandrosterone sulphate (DHEAS) were all measured at the SRL Laboratory (Tokyo, Japan). For testosterone, an electrochemiluminescence immunoassay was applied (ECLusys testosterone; Roche Diagnostics KK, Tokyo, Japan) and radioimmunoassays were used for DHEA and DHEAS (DPC DHEA and DPC DHEAS kits; Diagnostic Products Corporation, Los Angeles, CA, USA). The detection limits for testosterone, DHEA, and DHEAS were 5, 0.2, and 20 ng ml^{-1}, respectively. Inter- and intra-assay coefficients of variation were 6 and 8% for testosterone, 8 and 9% for DHEA, and 4 and 4% for DHEAS, respectively.

Appropriate ethical review boards approved the study, which followed the recommendations of the Declaration of Helsinki for biomedical research involving human subjects.

Statistical analysis

A paired *t*-test was used to compare the androgen levels between the two time periods. Patients were grouped into responders (CR and PR) and nonresponders (SD and PD) and the variables in each group were compared with an unpaired *t*-test. All statistical analyses were performed using SPSS version 8 statistical software (SPSS Inc., IL, USA).

RESULTS

Patient characterisation

Data for patient characteristics are listed in Table 1. Of the 67, 31 (46.3%) were women. The median age was 61 years (range, 42–80 years). There were 26 patients (38.8%) who had never smoked and adenocarcinoma was the primary histological finding in 56 cases (83.6%). There was no prior chemotherapy in 16 (23.9%) of the patients, and the remainder had received platinum-based chemotherapy.

Response to treatment could only be evaluated in 64 of the 67 cases. We observed 20 PR (29.8%), and of these, 13 (65%) were women and seven (35%) were men ($P = 0.074$). The median and range of treatment duration with gefitinib were 2.1 and 0.2–21 months. In all, 10 (50%) of 20 responders and 29 (66%) of 44 nonresponders had a smoking history ($P = 0.226$).

Effects of gefitinib treatment on androgens levels in NSCLC patients

Testosterone, DHEA, and DHEAS were detected in the serum of all 67 patients (see Table 2). There was a significant difference observed between men and women for serum testosterone levels ($P < 0.0001$), but not for serum DHEA or DHEAS (DHEA; $P = 0.267$, DHEAS; $P = 0.0565$).

In women, testosterone, DHEA, and DHEAS levels at pretreatment were significantly higher than during treatment (testosterone; $P = 0.025$, DHEA; $P = 0.0065$, DHEAS; $P = 0.0326$). In men, pretreatment testosterone and DHEA levels were significantly higher than during treatment, but there was no significant difference for DHEAS (testosterone, $P = 0.0009$; DHEA, $P = 0.0085$; DHEAS, $P = 0.33$). In addition, we compared hormone levels between smokers and nonsmokers. Pretreatment, there were no significant differences between women with and without a smoking history. On the other hand, hormone levels were significantly suppressed by gefitinib treatment in the 21 women who had no smoking history (testosterone, $P = 0.0016$; DHEA,

Table 1 Patient characteristics

Variable	No. of patients	%
Total	67	
Sex		
Male	36	53.7
Female	31	46.3
Age (years)		
Median	61	
Range	42–80	
Smoking history		
Never	26	38.8
Former/current	41	61.2
Performance status		
0, 1	48	71.6
≥2	19	28.4
Histology		
Ad	56	83.6
Non Ad	11	16.4
Stage		
II, IIIb	17	25.4
IV	27	40.3
Recurrence after surgery	23	34.3
Response		
PR	20	29.8
SD/PD	44	64.7
NE	3	4.5
Prior chemotherapy		
No	16	23.9
Yes	51	76.1

Ad = adenocarcinoma; non Ad = nonadenocarcinoma; PR = partial response; SD = stable disease; PD = progressive disease; NE = not evaluable

Table 2 Androgen levels in patients treated with gefitinib

	Pretreatment		During treatment		
Variable	***n***	**Mean ± s.d.**	***n***	**Mean ± s.d.**	**Paired t test**
Testosterone (ng ml^{-1})					
Female	31	215 ± 120	31	138.0 ± 110	$P = 0.025$
Male	36	1097 ± 1298	36	350.8 ± 1357	$P = 0.0009$
DHEA (ng ml^{-1})					
Female	31	2.21 ± 2.03	31	1.33 ± 0.83	$P = 0.0065$
Male	36	1.78 ± 1.06	36	1.49 ± 0.92	$P = 0.0085$
DHEAS (ng ml^{-1})					
Female	31	854.4 ± 579.5	31	645.8 ± 465.6	$P = 0.0326$
Male	36	1137.4 ± 607.7	36	1103.6 ± 601.5	$P = 0.33$

s.d. = standard deviation; DHEA = dehydroepiandrosterone; DHEAS = dehydroepiandrosterone sulphate

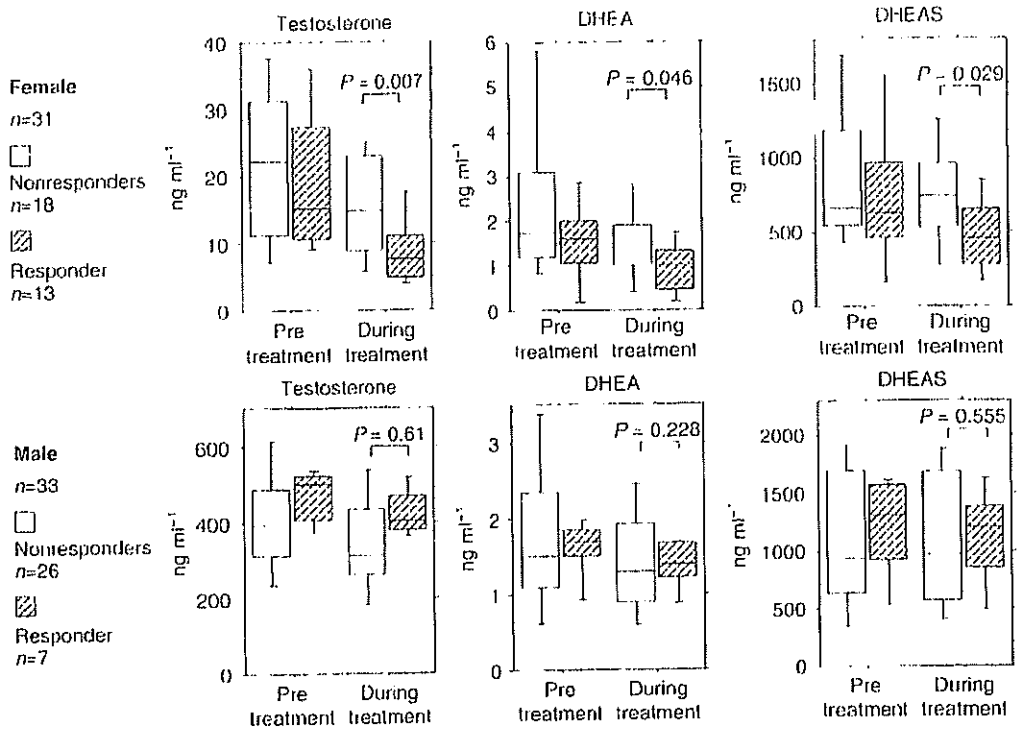

Figure 1 Serum testosterone, DHEA, and DHEAS levels, pretreatment and during the gefitinib administration. Each androgen levels are depicted in accordance to clinical response of gefitinib treatment (responders, PR; nonresponders, SD or PD). Error bars showed standard deviation.

$P = 0.0157$; DHEAS, $P = 0.0441$), but not in the 10 who had a smoking history (testosterone, $P = 0.6159$; DHEA, $P = 0.2487$; DHEAS, $P = 0.4740$). Figure 1 depicts the androgen levels for women after dividing the group into responders *vs* nonresponders. Testosterone, DHEA, and DHEAS levels in women responders during treatment were significantly lower than those observed in women nonresponders (testosterone, $P = 0.007$; DHEA, $P = 0.046$; DHEAS, $P = 0.029$). When men were included in the analysis, DHEA and DHEAS levels during treatment in the responders ($n = 20$) were still significantly lower than in the nonresponders ($n = 44$) (DHEA, $P = 0.0324$; DHEAS, $P = 0.0447$).

DISCUSSION

The present study of androgen levels (testosterone, DHEA, and DHEAS) in advanced NSCLC patients treated with gefitinib monotherapy revealed treatment-related decrease, especially in women who had no smoking history. The clinical response of gefitinib treatment appeared to be correlated with the suppression of the hormone levels.

To our knowledge, there have been no previous reports of effects of gefitinib treatment on levels of androgens in patients, although a number of authors have examined relationships between androgens and activity of the epidermal growth factor network (Klein and Nielsen, 1993; Dammann *et al*, 2000; Torring *et al*, 2003). There is evidence that EGFR expression is involved in prostate cancer development and in progression to androgen independence (Di Lorenzo *et al*, 2002), and an *in vitro* study has provided evidence that androgens increase the EGFR levels in androgen-sensitive prostate cancer cells and that EGFR signaling is essential for androgen induced proliferation and survival (Torring *et al*, 2003). Although there has been no indication of any relationship between androgens and EGFR in NSCLCs, expression of ARs has been detected in NSCLC cell lines and biopsy samples of primary lung cancers (Kaiser *et al*, 1996). Additionally, expression has been detected more frequently in women with adenocarcinoma, and thus this may be a prognostic factor for use of gefitinib in NSCLCs (Fukuoka *et al*, 2003; Kris *et al*, 2003; Miller *et al*, 2004). The data suggest that there is a correlation between the AR and EGFR functions in lung cancer. In agreement with this hypothesis, our results demonstrated clinical responses to gefitinib treatment to correlate with suppression of androgen levels.

One reason for lower androgen levels in responders than nonresponders might be that smokers are resistant and have higher androgen levels. However, there were no significant difference in smoking history between responders and non-responder in our study and there was no significant difference of the pretreatment levels of androgens between smokers and nonsmokers. On the other hand, gefitinib treatment significantly suppressed androgen levels in women who had no smoking history, but not in smokers. Smoking may disrupt the correlation between EGFR and androgen.

Both gefitinib and androgens are metabolised by CYP3A4/5; therefore, it can be speculated that gefitinib may affect the metabolisms of androgens. On the other hand, there are no direct evidences demonstrating PK interaction between gefitinib and androgens. PK interaction between gefitinib and other drugs metabolised by CY3A4/5 such as docetaxel or irinotecan were reported (Fandi *et al*, 2003; Furman *et al*, 2004). These reports suggested that gefitinib may decrease the clearance of these drugs and it may be due to CYP3A4/5 substrate competition. If there are any PK interactions between gefitinib and androgens, androgens clearance may decrease and androgen levels may increase by gefitinib treatment. However, we showed that gefitinib treatment decreased the levels of androgens and it suggested that the effect may not be due to change of CYP3A4/5 activity.

With single estimations of testosterone and DHEA, it is necessary to take into account the circadian rhythms. In this study, all blood was therefore taken at approximately the same time, that is, between 10:00 and 14:00, although this does not preclude any influence of cycles. On the other hand, several reports have suggested that there is no circadian rhythm for serum DHEAS levels (Molta and Schwartz, 1986; Hall *et al*, 1993; Kos-Kudla *et al*, 2001). Therefore, the differences seen in the DHEAS levels in this study presumably reflect actual effects of gefitinib treatment. This would suggest that the data for the other hormones might also have clinical significance.

In conclusion, the results of the present small, retrospective study indicate that androgen levels in NSCLC patients are affected by gefitinib treatment and that they may be factors determining sensitivity to this chemotherapeutic agent. Further large-scale prospective trials are needed in the future to confirm these results and to examine inter-relationships among androgens, smoking, gefitinib sensitivity, and EGFR mutations.

ACKNOWLEDGEMENTS

A part of this study was supported by Grants-in-Aid for Scientific Research from the Ministry of Education, Culture, Sports, Science, and Technology of Japan, and Grants-in-Aid for Cancer Research from the Ministry of Health, Labour, and Welfare of Japan.

REFERENCES

Beattie CW, Hansen NW, Thomas PA (1985) Steroid receptors in human lung cancer. *Cancer Res* 45: 4206 - 4214

Dammann CE, Ramadurai SM, McCants DD, Pham LD, Nielsen HC (2000) Androgen regulation of signaling pathways in late fetal mouse lung development. *Endocrinology* 141: 2923 - 2929

Di Lorenzo G, Tortora G, D'Armiento FP, De Rosa G, Staibano S, Autorino R, D'Armiento M, De Laurentiis M, De Placido S, Catalano G, Bianco AR, Ciardiello F (2002) Expression of epidermal growth factor receptor correlates with disease relapse and progression to androgen-independence in human prostate cancer. *Clin Cancer Res* 8: 3438 - 3444

Fandi A, Gatzemeier U, Smith R, Averbuch S, Manegold C (2003) Final data from a pilot trial of gefitinib (ZD1839) in combination with docetaxel in patients with advanced or metastatic non small-cell lung cancer (NSCLC): Safety and pharmacokinetics. *Proc Am Soc Clin Oncol* 22: 655

Ferlay J, Bray F, Pisani P, Parkin DM (2001) *GLOBOCAN 2000: Cancer Incidence, Mortality and Prevalence Worldwide, Version 1.0 (IARC, CancerBase No. 5)*. Lyon, France: IARC Press

Fukuoka M, Yano S, Giaccone G, Tamura T, Nakagawa K, Douillard J Y, Nishiwaki Y, Vansteenkiste J, Kudoh S, Rischin D, Eek R, Horai T, Noda K, Takata I, Smit E, Averbuch S, Macleod A, Feyereislova A, Dong R-P, Baselga J (2003) Multi-institutional randomized phase II trial of gefitinib for previously treated patients with advanced non-small-cell lung cancer. *J Clin Oncol* 21: 2237 - 2246

Furman WL, Daw NC, Crews KR, Stewart CF, McCarville B, Santana VM, Hawkins D, Rodriguez-Galindo C, Navid F, Houghton PJ (2004) A phase I study of gefitinib and irinotecan (IRN) in pediatric patients with refractory solid tumors. *Proc Am Soc Clin Oncol* 22: 8521

Hall GM, Perry LA, Spector TD (1993) Depressed levels of dehydroepiandrosterone sulphate in postmenopausal women with rheumatoid arthritis but no relation with axial bone density. *Ann Rheum Dis* 52: 211 - 214

Kaiser U, Hofmann J, Schilli M, Wegmann B, Klotz U, Wedel S, Virmani AK, Wollmer E, Branscheid D, Gazdar AF, Havemann K (1996) Steroid-hormone receptors in cell lines and tumor biopsies of human lung cancer. *Int J Cancer* 67: 357 - 364

Klein JM, Nielsen HC (1993) Androgen regulation of epidermal growth factor receptor binding activity during fetal rabbit lung development. *J Clin Invest* 91: 425 - 431

Kos-Kudla B, Ostrowska Z, Marek B, Ciesielska-Kopacz N, Kudla M, Kajdaniuk D, Siemidska L, Strzelczyk J (2001) Circadian serum levels of dehydroepiandrosterone sulphate in postmenopausal asthmatic women before and after long term hormone replacement. *Endocr Regul* 35: 217 - 222

Kris MG, Natale RB, Herbst RS, Lynch Jr TJ, Prager D, Belani CP, Schiller JH, Kelly K, Spiridonidis H, Sandler A, Albain KS, Cella D, Wolf MK, Averbuch SD, Ochs JJ, Kay AC (2003) Efficacy of gefitinib, an inhibitor of the epidermal growth factor receptor tyrosine kinase, in symptomatic patients with non-small cell lung cancer: a randomized trial. *JAMA* 290: 2149 - 2158

Law MR, Cheng R, Hackshaw AK, Allaway S, Hale AK (1997) Cigarette smoking, sex hormones and bone density in women. *Eur J Epidemiol* 13: 553 - 558

Lin P, Chang JT, Ko JL, Liao SH, Lo WS (2004) Reduction of androgen receptor expression by benzo[alpha]pyrene and 7, 8-dihydro-9, 10-epoxy-7, 8, 9, 10-tetrahydrobenzo [alpha] pyrene in human lung cells. *Biochem Pharmacol* 67: 1523 - 1530

Lynch TJ, Bell DW, Sordella R, Gurubhagavatula S, Okimoto RA, Brannigan BW, Harris PL, Haserlat SM, Supko JG, Haluska FG, Louis DN, Christiani DC, Settleman J, Haber DA (2004) Activating mutations in the epidermal growth factor receptor underlying responsiveness of non-small-cell lung cancer to gefitinib. *N Engl J Med* 350: 2129 - 2139

Miller VA, Kris MG, Shah N, Patel J, Azzoli C, Gomez J, Krug LM, Pao W, Rizvi N, Pizzo B, Tyson L, Venkatraman E, Ben-Porat L, Memoli N, Zakowski M, Rusch V, Heelan RT (2004) Bronchioloalveolar pathologic subtype and smoking history predict sensitivity to gefitinib in advanced non-small-cell lung cancer. *J Clin Oncol* 22: 1103 - 1109

Molta L, Schwartz U (1986) Gonadal and adrenal androgen secretion in hirsute females. *Clin Endocrinol Metab* 15: 229 - 245

Non-Small Cell Lung Cancer Collaborative Group (1995) Chemotherapy in non-small cell lung cancer: a meta-analysis using updated data on individual patients from 52 randomised clinical trials. Non-small Cell Lung Cancer Collaborative Group. *BMJ* 311: 899 - 909

Paez JG, Janne PA, Lee JC, Tracy S, Greulich H, Gabriel S, Herman P, Kaye FJ, Lindeman N, Boggon TJ, Naoki K, Sasaki H, Fujii Y, Eck MJ, Sellers WR, Johnson BE, Meyerson M (2004) EGFR mutations in lung cancer: correlation with clinical response to gefitinib therapy. *Science* 304: 1497 - 1500

Pao W, Miller V, Zakowski M, Doherty J, Politi K, Sarkaria I, Singh B, Heelan R, Rusch V, Fulton L, Mardis E, Kupfer D, Wilson R, Kris M, Varmus H (2004) EGF receptor gene mutations are common in lung cancers from 'never smokers' and are associated with sensitivity of tumors to gefitinib and erlotinib. *Proc Natl Acad Sci USA* 101: 13306 - 13311

Schiller JH, Harrington D, Belani CP, Langer C, Sandler A, Krook J, Zhu J, Johnson DH (2002) Comparison of four chemotherapy regimens for advanced non-small-cell lung cancer. *N Engl J Med* 346: 92 - 98

Torring N, Dagnaes-Hansen F, Sorensen BS, Nexo E, Hynes NE (2003) ErbB1 and prostate cancer: ErbB1 activity is essential for androgen-induced proliferation and protection from the apoptotic effects of LY294002. *Prostate* 56: 142 - 149

Trummer H, Habermann H, Haas J, Pummer K (2002) The impact of cigarette smoking on human semen parameters and hormones. *Hum Reprod* 17: 1554 - 1559

Wakeling AE, Guy SP, Woodburn JR, Ashton SE, Curry BJ, Barker AJ, Gibson KH (2002) ZD1839 (Iressa): an orally active inhibitor of epidermal growth factor signaling with potential for cancer therapy. *Cancer Res* 62: 5749 - 5754

WHO (1979) *World Health Organization: WHO Handbook for Reporting Results of Cancer Treatment*. Vol 48. Geneva, Switzerland: WHO Offset Publication